universität wien

DIPLOMARBEIT

Titel der Diplomarbeit

Early Effects of C-Raf Ablation in Liver Regeneration Upon a Toxic Insult

angestrebter akademischer Grad

Magister/Magistra der Naturwissenschaften (Mag. rer.nat.) bzw.
Magister/Magistra der Pharmazie (Mag.pharm.)

Verfasserin / Verfasser:	Matthias Parrini
Studienrichtung /Studienzweig (lt. Studienblatt):	A 490 Diplomstudium Molekulare Biologie UniStG
Betreuerin / Betreuer:	Prof. Dr. Manuela Baccarini

Wien, im November 2010

Table of Contents

I. Abstract

The Raf/MEK/ERK pathway comprises a signaling network involved in vital cell processes such as proliferation, apoptosis and differentiation and is tightly linked to cancer development and maintenance. Raf, the entry point of the ERK cascade, is present in three different isoforms, A-, B-, and C-Raf, each with distinct biological functions.

C-Raf is found over-expressed in a subset of human cancers, with particularly high frequency in hepatocellular carcinoma, the most frequently observed liver malignancy worldwide. Counterintuitively, hepatocyte-restricted ablation of the *c-raf* gene enhanced chemically-induced hepatocarcinogenesis in mice. This phenotype was rescued upon simultaneous *c-raf* ablation in hepatocytes and non-parchenchymal liver cells (liver-restricted knock out), indicating that C-Raf has different, cell-type specific roles in chemically-induced liver carcinogenesis. The tumor suppressing effect of C-Raf observed in hepatocyte-restricted ablation was ascribed to its role in the initiation phase of tumor development, since not only tumor load but also tumor multiplicity was higher in hepatocyte-restricted *c-raf* knock out mice, indicating an elevated level of initiated cells, thus a higher initial susceptibility to chemical induced carcinogenesis. To gain insight in the differences between hepatocyte-restricted *c-raf* ablation and ablation in both parenchymal and non parenchymal liver cells we compared the reaction of the animals immediately after the application of the carcinogen. These short-term experiments unveiled enhanced lipid droplet accumulation, prolonged STAT3 signaling and a delayed proliferative response in hepatocyte-restricted *c-raf* knock out mice. In the animals with *c-raf* ablation in liver parenchymal and non-parenchymal cells these effects could not be observed. Liver-restricted *c-raf* ablation was induced by the administration of Poly I:C, which triggered Cre recombinase expression and gene ablation, ten days prior to the induction of chemical carcinogenesis. Since Poly I:C induces an inflammatory state in the liver, and since inflammation is tightly interlinked with hepatocarcinogenesis, we sought to determine whether this treatment interfered with liver cancer development in our carcinogenesis protocol.

We could show that Poly I:C interfered with the induction of apoptosis and with the production pattern of the pro-tumorigenic cytokine IL-6 following carcinogen treatment *in vivo*.

II. Zusammenfassung

Der Raf/MEK/ERK Signaltransduktionsweg ist ein essentielles Netzwerk, dass zur Informationsverarbeitung von der Zelle benutzt wird um lebenswichtige Prozesse wie Wachstum, programmierten Zelltod und Zelldifferenzierung zu regulieren und aufeinander abzustimmen. Diese Signalkaskade wurde in der Vergangenheit schon oft mit der Entstehung von Krebs assoziiert und ist Gegenstand derzeitiger Krebsforschung. Raf, die erste Kinase des ERK-Transduktionsweges, existiert in Säugetieren in drei verschiedenen Isoformen, A-, B- und C-Raf, wobei jede einzelne einer individuellen biologischen Funktion nachgeht.

Im Rahmen der Entstehung bestimmter Karzinome wurde eine Überexprimierung von C-Raf festgestellt. Besonders im Zusammenhang mit dem hepatozellulärem Karzinom, dem weltweit häufigsten Lebermalignom, konnte eine aberrante Expression dieses Proteins nachgewiesen werden, was auf eine Funktion als Tumorpromoter hinweist. Hepatozyten-spezifischer *c-raf* Knock-out in Mäusen in Verbindung mit chemisch induzierter Karzinogenese wies eine tumorsupprimierende Wirkung von C-Raf auf, da *c-raf* Knock-out Mäuse eine erhöhte Inzidenz an Lebertumoren zeigten. Dieser Phenotyp konnte mit zeitgleicher Deletion von *c-raf* in Hepatozyten und nicht-parenchymalen Zellen (leber-spezifischer Kock-out) aufgehoben werden, was wiederum auf eine zelltypische Funktionsweise von C-Raf bei chemisch-induzierter Karzinogenese deutet.

Der tumorsupprimierende Effekt von C-Raf im Hepatozyten-spezifischen Knock-out scheint sich hauptsächlich in der Initiationsphase vom hepatozellulärem Karzinom auszuwirken, da sowohl die Tumorgröße als auch die Tumormultiplizität in hepatozyten-spezifischen *c-raf* Knock-out Mäusen höher war. Dies erklärt sich durch eine erhöhte Suszeptibilität für chemisch induzierte Karzinogenese und somit einer erhöhten Anzahl an initiierten Zellen. Um einen Einblick in die Unterschiede zwischen hepatozyten-spezifischem *c-raf* Knock-out und der Deletion von *c-raf* sowohl in Hepatozyten als auch in nicht-parenchymalen Zellen zu erhalten, wurde die Reaktion der Tiere sofort nach der Applikation des Karzinogens vergli-

chen. Diese vergleichenden Analysen enthüllten eine erhöhte Akkumulation von Fetttröpfchen (Steatose), eine erhöhte und verlängerte STAT3 Signalwirkung und eine Verzögerung der proliferativen Antwort in der Leber kurz nach Applikation des Kanzerogens in hepatozyten-spezifischen Knock-out Mäusen. In den Tieren mit einer Deletion von *c-raf* in Hepatozyten und nicht-parenchymalen Zellen konnte dieser Effekte nicht beobachtet werden.

Der leber-spezifischer *c-raf* Knock-out wurde durch die Injektion von Poly I:C induziert, womit die Expression der Cre Rekombinase und die Geneablation eingeleitet wurde, was 10 Tage vor der Applikation des Karzinogens statt fand. Poly I:C löst einen inflammatorischen Zustand in der Leber aus, und da Entzündung mit Hepatokarzinogenese zusammenhängt, versuchten wir eine mögliche Beeinflussung des Karzinogeneseprotokolls durch diese vorangehende Poly I:C Behandlung festzustellen. Tatsächlich konnte nach der Karzinogenapplikation ein Effekt von Poly I:C auf die Apoptose und das Expressionsmuster von IL-6 nachgewiesen werden.

III. Introduction

III.1 Cell signaling – We Need to Talk

Processing information is central for every living organism, and thus also to their basic constituents, the cells. Communication systems have evolved to guarantee a successful exchange of information enabling a living together – not only for us humans, but also for cells which do communicate by producing, releasing and recognizing chemical molecules. This process, referred to as signaling, is used by cells to exchange information and coordinate their basic activities, as well as, in multi-cellular organisms, to direct and control process such as tissue homeostasis, development and immunity. Failure within these complex transmission routes leads to diseases such as cancer or autoimmunity.

III.2 The MAPK paradigm

The evolutionary conserved mitogen-activated protein kinase (MAPK) pathway is one of the most important signal transduction modules. Communication starts as a signal recognized at the cell surface, which is further transmitted to the nucleus or elsewhere in the cell, where it regulates vital processes such as proliferation, differentiation, survival, apoptosis and cell motility. The general architecture of the MAPK pathway features a three-tiered cascade (Fig. 1A), composed of a MAPK kinase kinase (MAPKKK or MAP3K) typically activated by an upstream G-protein, which phosphorylates, thus activating, a MAPK kinase (MAPKK or MAPK2). The business end of the pathway, the MAPK, is phosphorylated by the MAP2K, and once activated phosphorylates numerous cytosolic and cytoskeletal substrates, thereby generating fast and transient changes in metabolism and cell-shape. Further, durable changes can be triggered by translocation of activated MAPKs into the nucleus, where they interact with nuclear transcription factors to change gene expression pattern of the cell (Niault and Baccarini 2010). Inactivation of this cascade is achieved by dephosphorylation of these three kinases via

specific phosphatases, referred to as MAPK phosphatases (Chang and Karin 2001; Baccarini 2005; Orton et al. 2005; Niault and Baccarini 2010).

The MAPK signaling system is capable of amplifying the signal at each stage. In addition, parameters such as kinetics, duration and amplitude of activity can be regulated separately for each tier (Kolch 2000). It is important to mention that MAPK pathways, although originally described as linear and unidirectional, are competent to interact with members of other pathways through kinase-dependent and/or kinase-independent functions (Hindley and Kolch 2002; Baccarini 2005). These processes are referred to as signal cross talk.

To date, four functionally distinct MAPK pathways have been elucidated with four terminal MAPKs, which are eponymous for these cascades: extracellular signal regulated kinase (ERK-1/2), Jun amino-terminal kinases (JNK-1/2/3), p38 (α/β/γ/δ) and ERK5 (Chang and Karin 2001). Each of these MAPKs can be activated not only by one MAP2K, but rather by diverse MAP2Ks, and that this scheme applies also on the level of MAP3Ks, clearly illustrates the intrinsic complexity of this signal transduction paradigm.

III.3 The Raf/MEK/ERK pathway

The ERK pathway was one of the first pathways to be described, providing a roadmap for signals coming from the cell surface and being transduced to the nucleus. This pathway has been extensively studied and features Raf (rapidly growing fibrosarcoma) as MAP3K, MEK (MAPK and ERK kinase) as MAP2K and finally ERK as MAPK (Fig. 1B). Extracellular signals trigger this pathway by activating growth factor receptors (receptor tyrosine kinases - RTKs), leading to the assembly of receptor cell signaling complexes including the adaptor proteins Grb (growth factor receptor bound protein) 2 and Shc (Src homology and collagen homology). Through the activation of SOS (son of sevenless), a GDP/GTP exchange factor (GEF), and the subsequent exchange of Ras-bound GDP with GTP, the small GTPase Ras (rat sarcoma) changes into its active confirmation, thus

recruiting Raf to the inner cell membrane. Raf is activated by direct interactions with Ras and by a rather complex, not fully understood process including phosphorylation, dephosphorylation and changes in conformation. Further down the pathway, activated Raf phosphorylates its downstream target MEK, which will in turn phosphorylate ERK (Orton et al. 2005). This terminal MAPK has at least 180 known substrates in nucleus and cytoplasm (Yoon and Seger 2006) making it the kinase with the largest assortment of effectors (Niault and Baccarini 2010). The ERK pathway is attenuated after activation by negative feedback loops implemented by ERK and shut down by sequential dephosphorylation of activating residues on Raf, MEK and ERK (Niault and Baccarini 2010).

Mammals have two distinct *erk* genes (*erk 1/2*), two *mek* genes (*mek 1/2*) and three *raf* genes (*a-*, *b-* and *c-raf* also *c-raf-1*). Each level of the ERK pathway consists of more than one component, accounting for increased flexibility via hetero- and homodimerization and individual biological functions. C-Raf and B-Raf form heterodimers upon Ras activation, resulting in a higher MEK kinase activity compared to the single constituents or homodimers (Weber et al. 2001; Garnett et al. 2005; Rushworth et al. 2006). Further, MEK1 and MEK2 heterodimers are significantly involved in the fine tuning of the pathway (Catalanotti et al. 2009), and ERK homodimers are important for spatial specificity (Casar et al. 2008).

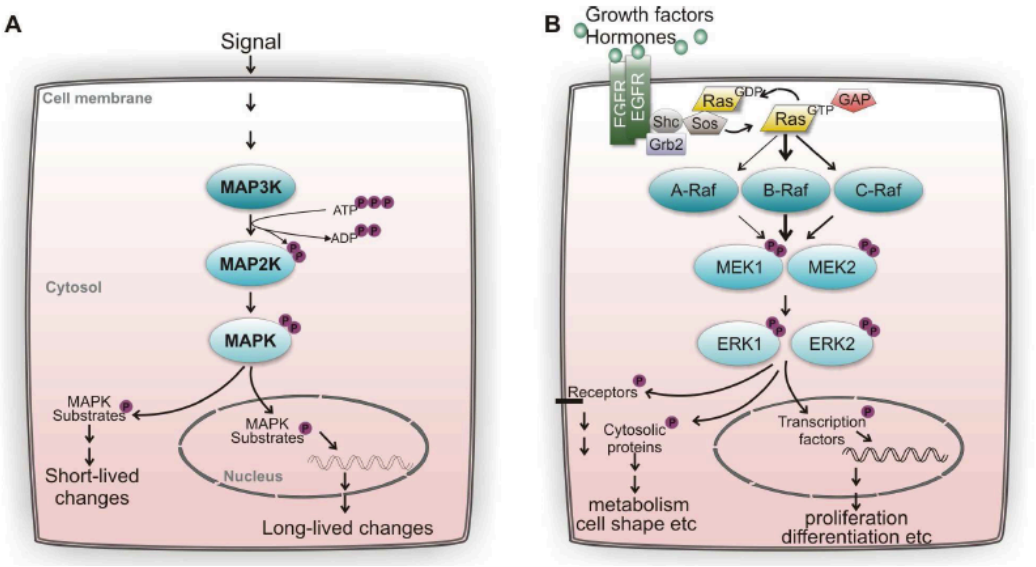

Figure 1. The MAPK Pathway and the Raf/MEK/ERK pathway, adapted form (Niault and Baccarini 2010)

A) The MAPK pathway: general assembly of a three-tiered MAPK cascade including the three kinases MAP3K, MAP2K and MAPK. Upon activation each kinase passes the signal on to its downstream target via phosphorylation (P for phosphate group). The activated MAPK triggers short-lived changes by phosphorylation of cytosolic substrates and long-lived changes by phosphorylation of nuclear targets influencing gene expression. B) The Raf/MEK/ERK pathway: upon receptor stimulation by growth factors and hormones, the Raf/MEK/ERK cascade initiates and proceeds towards its business end ERK. Adaptor proteins (Grb2, Shc) recruit the GDP/GTP exchange factor SOS, which in turn activates the small GTPase Ras. Raf becomes then activated by Ras, transmitting the signal by phosphorylation further to its downstream target MEK. Activated MEK phosphorylates ERK, rendering it able to activate its various substrates. B-Raf has been shown to be the most potent MEK activator, as is illustrated by the thickness of the arrows.

The distinct biological functions of kinases belonging to the same tier of the cascade are illustrated best by the example of the MAP3Ks A-Raf, B-Raf and C-Raf. All three Raf isoforms feature a common structure with three conserved regions (CR1, CR2, CR3) (Fig. 2). CR1 and CR2, both part of the regulatory domain, are located in the N-terminus, whereas CR3, harboring the kinase domain, is located in the C-terminus. CR1 consists of a Ras-binding site (Galabova-Kovacs et al.) and a cystein-rich domain (CRD), which are needed for membrane recruitment

(Ras binding site) and autoinhibition (CRD). CR2 features a multitude of negative regulatory phosphorylation sites, including a negative regulatory serine residue (Wellbrock et al. 2004; Niault and Baccarini 2010). Considering these structural and functional similarities, one could be misled into believing that the three Raf proteins are functionally redundant. Instead, biochemical and in vivo studies (including knock-in and knock-out experiments) proved that each individual isoform has essential biological functions.

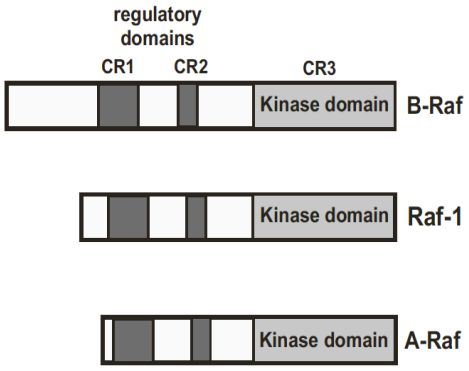

Figure 2. Structure of Raf isoforms, adapted from (Thiel et al. 2009)
A-, B- and Raf-1 (C-Raf) share three conserved regions: CR1 containing a cysteine rich domain and Ras-binding sub-domain for Ras-GTP binding, CR2 with numerous serine and threonine residues influencing the catalytic activity and CR3 harboring the kinase domain.

B-Raf is considered to be the main MEK activator, as its Ras binding and kinase activity were shown to be stronger than in the two other Raf isoforms (Pritchard et al. 1995; Marais et al. 1997; Galabova-Kovacs et al. 2006; Sobczak et al. 2008). The conventional ablation of B-Raf led to embryonic lethality around midgestation, as a result of reduced vascular development in the placenta. Deletion of B-Raf in the embryo itself (ablation in the epiblast compartment) yielded viable offspring, which died around three weeks after birth because of neurological defects (Galabova-Kovacs et al. 2006).

Conditional ablation of B-Raf (for details about knockout models see below) in several tissues and cell types e.g. in brain, where B-Raf is preferentially expressed (Chen et al. 2006; Galabova-Kovacs et al. 2008), thymocytes (Tsukamoto et al. 2008) and endothelial cells (Wimmer et al., unpublished data) leads to tissue-specific phenotypes, including decreased MEK and ERK phosphorylation and

therefore attenuation of signal processing through the ERK pathway, reinforcing B-Raf's status as main activator of MEK (Niault 2009).

Conventional *c-raf* ablation results, as the *b-raf* deletion, in embryonic lethality during midgestation. Embryos lacking *c-raf* are retarded in growth, display vascularization defects in placenta and the yolk sac, and show increased apoptosis especially in the fetal liver, while proliferation was unchanged (Huser et al. 2001; Mikula et al. 2001). These results showed that C-Raf is essential for preventing apoptosis rather than for promoting proliferation (Piazzolla et al. 2005), thereby breaking new ground within this signaling pathway.

Conditional *c-raf* knockouts and biochemical studies led to deeper understanding, revealing kinase-independent functions of C-Raf and providing new insights into its function in pathway cross-talk. Two pro-apoptotic kinases were identified so far as C-Raf interaction partners: mammalian sterile 20 (Ste20)-like protein kinase 2 (MST2), involved in the regulation of the Lats/YAP pathway (O'Neill et al. 2004), and apoptosis signal-regulating kinase 1 (ASK1), regulating apoptosis triggerd by death receptors or stress, functioning upstream of JNK and p38 (Chen et al. 2001; Yamaguchi et al. 2004; Baccarini 2005). Both kinases, ASK1 and MST2, are inhibited through a kinase independent mechanism, involving complex-formation with C-Raf and inhibiting/modulating the target's kinase activity. Last but not least a third kinase, Rho kinase α (Rok-α), was brought to light as a C-Raf interaction partner. Rok-α is a cytoskeleton-based kinase engaged in migration, thereby influencing cell shape and motility (Baccarini 2005).

In contrast to B-Raf and C-Raf, A-Raf has been the less extensively studied MAP3K of the ERK pathway. Conventional knockout of the *a-raf* gene does not result in embryonic lethality. *a-raf* deficient mice are born normal but fail to thrive and die between P7 (*post partum*) and P21 displaying neurological and intestinal abnormalities. Depending on the genetic background, mice lacking the *a-raf* gene can also survive the adolescence and grow up with minor neurological defects (Pritchard et al. 1996). Thus, A-Raf is not required for embryonic development, yet it is possibly indispensible after birth.

Taken together, the Raf kinase family illustrates in an impressive manner that each protein has its own distinct and indispensable functions. In addition, expression of the three isoforms varies from tissue to tissue and localization within the cell differs (Barnier et al. 1995; Morice et al. 1999; Wojnowski et al. 2000) demonstrating again how complex and tunable MAPK pathways are.

III.4 Signaling Pathways and Cancer – Focusing on Ras and Raf

The term ”cancer”, defining diseases where a cluster of cells behave aberrantly, proliferating uncontrollably, invading surrounding tissue and in certain cases metastasizing to different regions of the body, was probably first introduced in Greece more than 2000 years ago by Hippocrates. Since then, knowledge about this class of diseases has grown continuously, especially in the last 35 years during which genetic alterations connected to cancer were identified (Graves 2000). In 2000, Hanahan and Weinberg published their famous review ‘*Hallmarks of Cancer*’ combining and integrating the plethora of information gathered up to that point and outlining the main features of cancer: cell-sufficiency in growth signals, evading apoptosis, insensitivity to anti-growth signals, limitless replicative potential, sustained angiogenesis, metastasis and tissue-invasion (Hanahan and Weinberg 2000). All these hallmarks are reflections of aberrant signaling by pathways controlling proliferation, apoptosis, differentiation and motility (Martin 2003). MAPK pathways have been shown to be almost indispensible for tumor formation, as numerous cancer types harbor mutations resulting in over-activation of the pathway and/or over-expression of its components (Ding et al. 2007).

Within the ERK pathway, *ras* and *b-raf* are the two genes most susceptible to activating mutations. With an average incidence of 33% in all human cancers, *ras* is the oncogene most frequently found mutated. These mutations are mostly localized to the Ras GTPase region and retain Ras in its active state, driving its downstream pathway continuously. *b-raf* mutations enhance predominantly the kinase

activity towards its sole substrate MEK, resulting again in increased ERK signaling. Less common mutations lower B-Raf kinase activity but increase its ability to form heterodimers with C-Raf, ultimately stimulating C-Raf's kinase activity and therefore the MEK/ERK pathway (Davies et al. 2002; Garnett et al. 2005; Niault and Baccarini 2010).

C-Raf is rarely mutated but is an aberrantly expressed protein present in a subset of different cancers. Over-expression of C-Raf is frequently observed in squamous cell carcinomas (Riva et al. 1995), lung adenocarcinomas (Cekanova et al. 2007) and hepatocellular carcinomas (Huynh et al. 2003; Hwang et al. 2004). Furthermore, C-Raf has been found to be essential for development and maintenance in Ras-driven skin tumors by inhibiting Rok-α through its kinase-independent functions (Ehrenreiter et al. 2009). The effect on several pathways simultaneously and the associated interference with processes such as differentiation and proliferation is evident, considering C-Raf's ability in cross-talking and its numbers of downstream targets, resulting finally in contribution to tumor development.

III.5 The Murine Liver: Hepatocelluar Carcinoma and *c-raf* – Vicious Love Birdies

The liver is the largest gland and the central metabolic organ of the body. Detoxification, glycogen storage, protein synthesis and hormone production are pivotal functions accomplished by this organ. Furthermore, the liver is responsible for bile production, an adjuvant in the digestion process. Anatomically, the liver is divided into lobes, the number of which varies among species. In rodents, the liver comprises one large and three smaller lobes.

Blood flow through the liver is essential for both oxygen supply and for its metabolic functions. Nutrient-enriched blood coming from the gastrointestinal tract (and to a considerably lower extent from spleen and pancreas) enters the liver through the *vena portae* (portal vein), whose numerous branches create a complex

vascular system (Fig 3A). Following the flow, the blood exits the portal veins into intrahepatic spaces, the sinusoids, collects again in the central veins and leaves the liver through the *vena hepaticae* (hepatic vein). A second vascular system, starting with the *arteria hepatica propria* (hepatic artery proper) and branching into hepatic arteries, runs through the liver ensuring the supply of oxygen and nutrients for the organ itself. Hepatic arteries are found next to portal veins, together with a bile duct, forming the portal triads. The basic structural unit of the liver is called lobule, not to be confounded with anatomical lobes, and comprises a central vein surrounded by six portal triads (Fig. 3B).

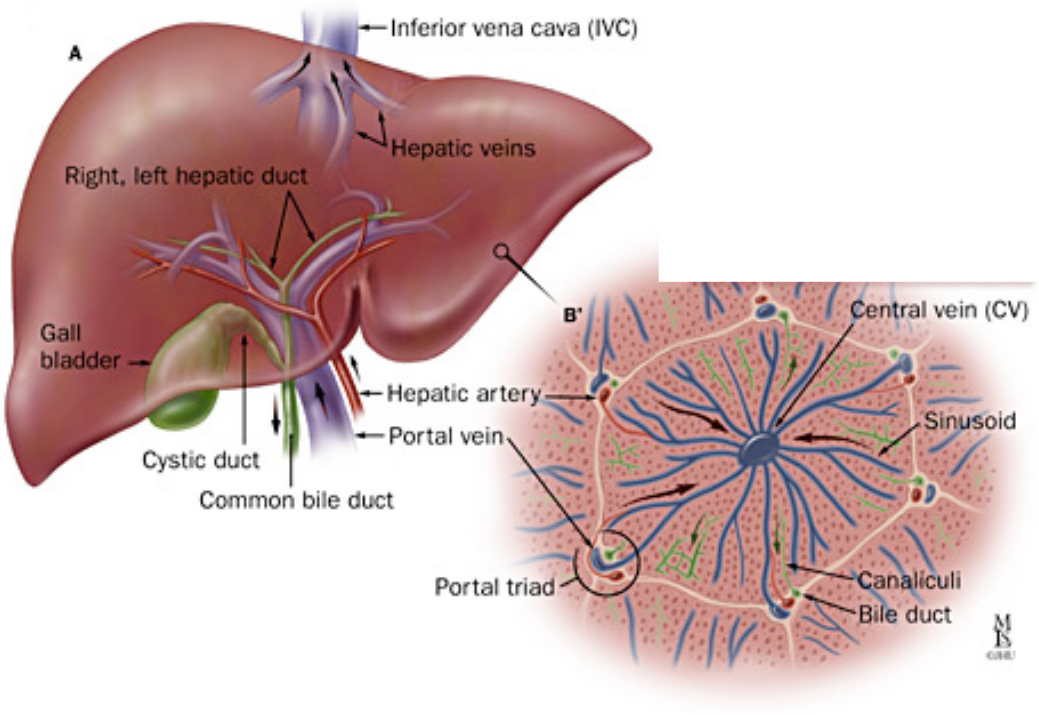

Figure 3. Hepatic vascular system and hepatic lobule, adapted from John Hopkins Medicine (www.hopkins-gi.org/Upload/200710290953_38845_000.jpg)

A) A schematic depiction of the hepatic blood supply system including the hepatic portal vein, the hepatic artery and the common bile duct. B) A schematic picture of the hepatic lobule with one central vein being surrounded by 6 portal triads. Blood flow (blue and red vessels) and bile flow (green vessels) are indicated by black arrows in both images.

Two portal triads and a central vein form a triangle referred to as acinus, which is considered the functional unit of the liver (Fig. 4). In the acinus, blood from the portal vein circulates into sinusoids, which are capillary-like blood vessels lined with interrupted endothelium containing the liver resident macrophages or Kupffer cells. Through gaps in the endothelium, termed fenestrae, blood seeps out of the sinusoids deeper into the tissue, the so-called Space of Disse. There it reaches the parenchymal cells of the liver, the hepatocytes, which take up and metabolize oxygen, nutrients and toxins.

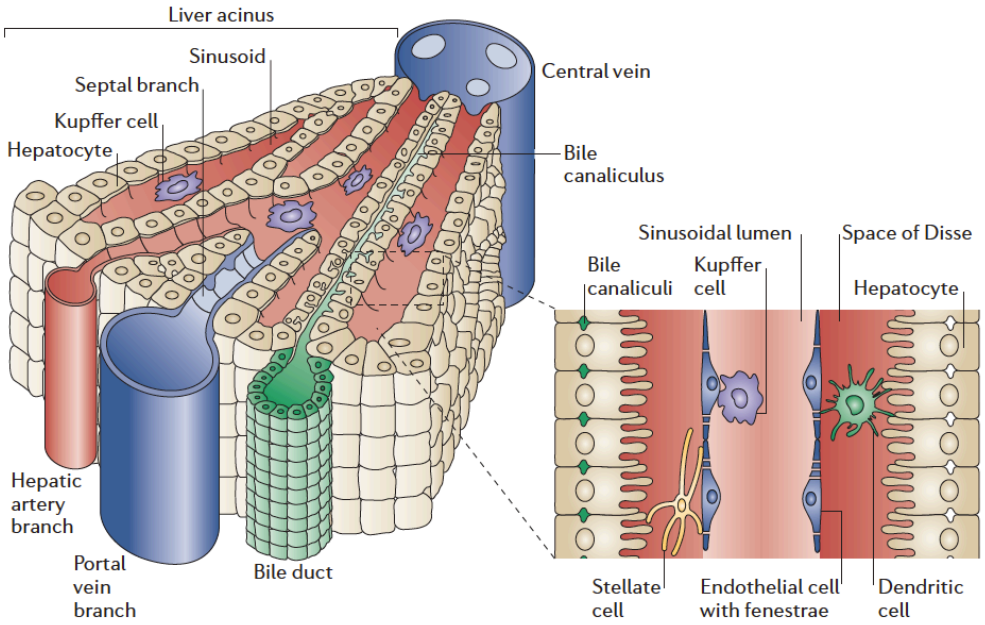

Figure 4. Structure of the liver acinus and sinusoids, adapted from (Adams and Eksteen 2006)

Portal veins and hepatic arteries ensure the blood supply of the liver. Blood from these vessels reaches the sinusoids, proceeds along the acinus and collects in the central vein. Sinusoids (depicted on the right) are small vessels lined with specific endothelial cells that have a unique morphology and phenotype. These cells are characterized by fenestrae (small interruptions of the endothelium) and the absence of tight junctions. The macrophages of the liver (Kupffer cells) reside in the sinusoids. The Space of Disse lies between the sinusoidal endothelium and the hepatocytes and hosts Ito cells (hepatic stellate cells) that store fat and vitamins, and dendritic cells.

As the main detoxifying organ of the body, the liver is confronted with metabolic and oxidative stress as well as immunological responses to pathogens on a regular basis. But since the dose makes the poison, chronic inflammation and excessive liver damage, triggered by various causes such as immoderate alcohol consump-

tion and hepatitis, can result in a variety of diseases such as steatosis, cirrhosis and cancer.

The most frequent primary liver disease worldwide is hepatocellular carcinoma (HCC), taking a toll of over 610.000 deaths per year (WHO 2009). Once HCC has been diagnosed, prognosis is very poor, enlisting this type of cancer among the top three of most lethal cancers (Parkin et al. 2001). The main reasons for this are late diagnosis and lack of effective treatments. Early HCC is hardly recognized since this disease is almost asymptotic and screening methods are unsatisfactory (Thomas and Abbruzzese 2005). In addition, treatment of HCC so far has very low success rates, due to the lack of effective therapeutics for patients suffering from advanced HCC (Whittaker et al. 2010).

Pathogenesis of HCC is complex involving on the one hand cirrhosis as a consequence of sustained tissue damage and on the other hand mutations in oncogenes and/or tumor suppressors. Cirrhosis is caused by infections (hepatitis), metabolic defects (e.g.: non-alcoholic steatohepatitis (NASH), obesity and type II diabetes) and toxins (e.g.: alcohol or aflotoxin B) and is characterized by fibrosis (replacement of parenchyma by connective tissue) and regenerative nodules (Whittaker et al. 2010). Several signaling networks – growth factor mediated signaling, MAPK pathways, AKT and WNT signaling, to name a few – have been closely associated with cirrhosis and HCC.

The RAF/MEK/ERK pathway is at the center of our interest since it has been proven to be constitutively active in HCC, with increased MEK 1/2 and ERK phosphorylation in tumor tissue compared to non-effected tissue (Ito et al. 1998; Huynh et al. 2003; Hwang et al. 2004). This seems to be dependent on two main mechanisms: activating *ras* mutations and constitutive activation of C-Raf by deregulated growth factor expression. Activating *ras* mutations have been found in HCC, percentages depending on the source varying from 4% (Catalog of Somatic Mutations in Cancer) to 30% (Whittaker et al. 2010). Furthermore, overexpression of *c-raf* has been found in 100% of human HCC samples (30 specimens analyzed by Hwang et al, 2004). In contrast, *b-raf* mutations seem to be

very rare in HCC (Tannapfel et al. 2003), which is particularly interesting because *b-raf* mutations are commonly observed in many other cancer types.

III.6 Inflammation, Regeneration and Liver Cancer – Kupffer Cells as Key Players

The relationship between cancer development and inflammation has been recognized since the nineteenth century. HCC is a prime example for an inflammation-associated cancer type, since chronic inflammation is invariably associated with this malignancy (Berasain et al. 2009). Hepatic inflammation is mediated mainly via Kupffer cells, which react to inflammatory stimuli. These liver resident macrophages derive from circulating monocytes, which develop out of progenitors from the bone marrow and differentiate into Kupffer cells when localizing to the liver. Apart from phagocytosis and antigen processing and presenting, Kupffer cells produce and release inflammatory mediators, reactive oxygen species and growth factors, which in turn influence endothelial cells, stellate cells and most importantly hepatocytes (Stienstra et al. 2010).

The interplay between Kupffer cells and hepatocytes has not yet been fully clarified, but two different scenarios have been proposed. The first involves Kupffer cells as primary responder to toxic signals, leading to the release of cytokines, which affect hepatocyte proliferation, survival and function. In some cases the activation of Kupffer cells has been shown to protect, yet in others to damage the parenchyma (Roberts et al. 2007). Roberts et al. (2007) hypothesized that the primary Kupffer cell response can shift from protective to damaging during prolonged inflammation (threshold hypothesis). In the second scenario the hepatocytes send signals forth to Kupffer cells, which in turn support hepatocyte survival and protect from apoptosis.

Hepatic inflammation entails liver damage, which is followed by liver regeneration. This process is based on the production of cytokines such as interleukin (IL) 6 and tumor necrosis factor (TNF) α, and of growth factors such as hepatocyte

growth factor (HGF), transforming growth factors (TGFs) and epidermal growth factor (EGF) (Taub 2004).

IL-6 and TNF-α are crucial for liver regeneration (Fig. 5). By activating the transcription factor nuclear factor kappa-light-chain-enhancer of activated B cells (NF-κB), TNF-α stimulates Kupffer cells to produce IL-6. Secreted IL-6 is recognized by hepatocytes through the corresponding IL-6 Receptor (IL-6R) initiating a cascade including association of two gp130 and activation of two Janus kinases (JAKs), cross-phosphorylation of JAKs and phosphorylation of signal transducer and activator of transcription (Stat) 3. Activated Stat3 dimerizes and translocates to the nucleus, where it activates genes involved in the so-called acute phase response (elimination of toxic or infectious agents), in liver regeneration and in hepatoprotection (protection against chronic liver injury). A second pathway activated by IL-6 is the MAPK pathway (especially ERK and JNK), considered vital for hepatocyte proliferation (Taub 2004).

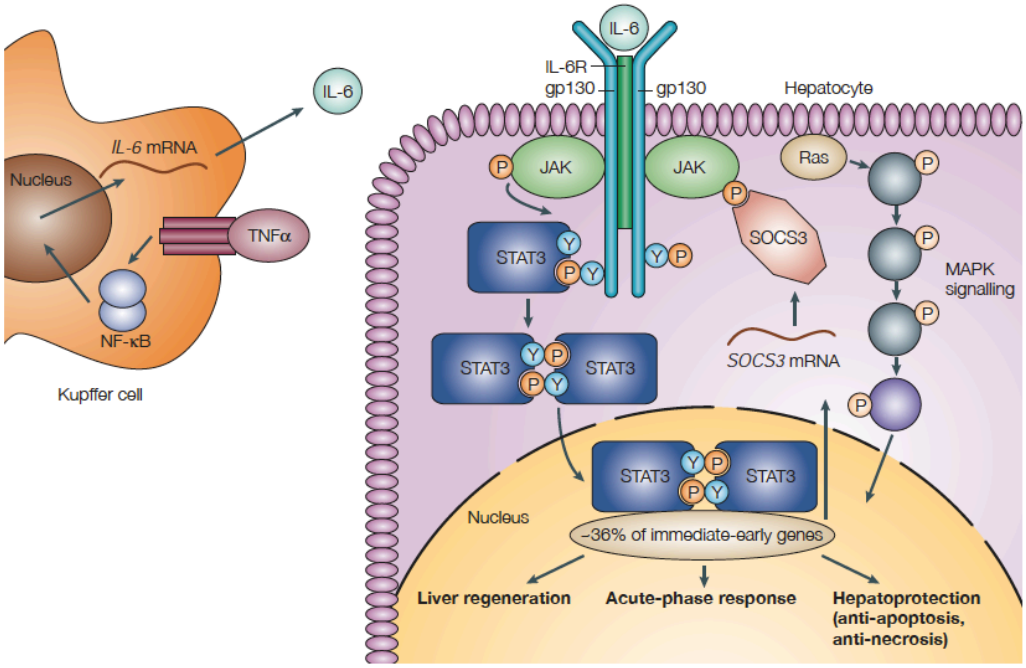

Figure 5. Stat3 signaling in liver regeneration, adapted from (Taub 2004)

TNF-α is recognized by KCs, which in turn activate NF-κB thereby triggering IL-6 expression. IL-6 binds to IL-6R resulting in the activation of JAKs. JAKs phosphorylate (P for phosphate group) Tyrosine residues on Stat3, which dimerizes and translocates to

the nucleus where it upregulates the transcription of immediate-early genes, thereby triggering the acute-phase response, hepatoprotection and liver regeneration. The second pathway activated through IL-6 is the MAPK pathway – for details see Fig. 1.

IL-6 is important in the acute phase response and hepatoprotection, but is not by itself sufficient to induce the process of liver regeneration (Cressman et al. 1996; Sakamoto et al. 1999). Growth factor-driven pathways stimulate the proliferative response upon liver injury, thereby supporting restoration and maintenance of liver function and architecture. HGF and TGF-α are regarded as the two most important growth factors in liver regeneration. Both growth factors are involved in activation of mitogenic pathways such as PI3K, ERK and AKT, and stimulate DNA synthesis and proliferation (Taub 2004).

III.7 Conditional Knock Out Systems

Conventional *c-raf* ablation results in embryonic lethality. Therefore, we use a conditional knock out system to target a particular cell type (tissue-restricted ablation) and/or a specific point in time (temporally controlled ablation). To achieve this, we use the site-specific Cre recombinase (Type I topoisomerase) from bacteriophage P1. The Cre recombinase recognizes and cuts specific DNA sequences, so called LoxP sites, resulting in the excision of the intervening sequences. If the LoxP sites are placed in introns flanking an essential exon, this causes the disruption of the floxed (flanked by Lox) gene (Fig. 6). The expression of the Cre recombinase is typically controlled by a tissue-restricted or by an inducible promoter (Rajewsky et al. 1996).

Several promoter systems are available for liver-restricted gene ablation. In this study, we used the Alfp promoter and the Mx1 promoter. The Alfp promoter derives from the albumin promoter (Alb) and consists of the mouse albumin enhancer, the albumin promoter and an α-fetoprotein enhancer. In Alfp-Cre transgenic mice recombinase expression starts around embryonic day (E) 10.5 and excision

of floxed DNA is observed specifically in hepatocytes and biliary epithelia cells (Kellendonk et al. 2000; Metzger 2004).

The Mx1 promoter is induced by interferons and is therefore activated in interferon sensitive cells, affecting a larger spectrum of cells than the Alfp promoter system. In Mx-Cre mice Cre expression is triggered via *intra peritoneal* (*i.p.*) injection of either interferon itself or PolyI:PolyC (double stranded RNA polymer), which induces interferon production by peritoneal macrophages. Ablation of floxed DNA segments is detected in liver to almost 100%, not only in hepatocytes but also in non-parenchymal cells such as hepatic stellate cells and Kupffer cells. Even though other tissues are also affected (to a lesser extent), this knock out model has been instrumental in elucidating gene functions in the liver (Kuhn et al. 1995; Metzger 2004).

Transgenic mice harboring the Cre recombinase are mated to animals carrying the floxed alleles of interest to generate a conditional knock-out line. In this study, we used a *c-raf* flox mouse line [*c-raf* $^{F/F}$], crossed to either the Alfp-Cre or the Mx-Cre mouse line, resulting in [*c-raf*$^{\Delta hep/\Delta hep}$; Alfp-Cre] or [*c-raf* $^{F/F}$; Mx-Cre], respectively. [*c-raf*$^{\Delta liv/\Delta liv}$; Mx-Cre] animals are obtained by Poly I:C application, which activates the transcription of the *Cre* gene. Efficient ablation of *c-raf* is achieved through Cre-mediated excision of exon 3.

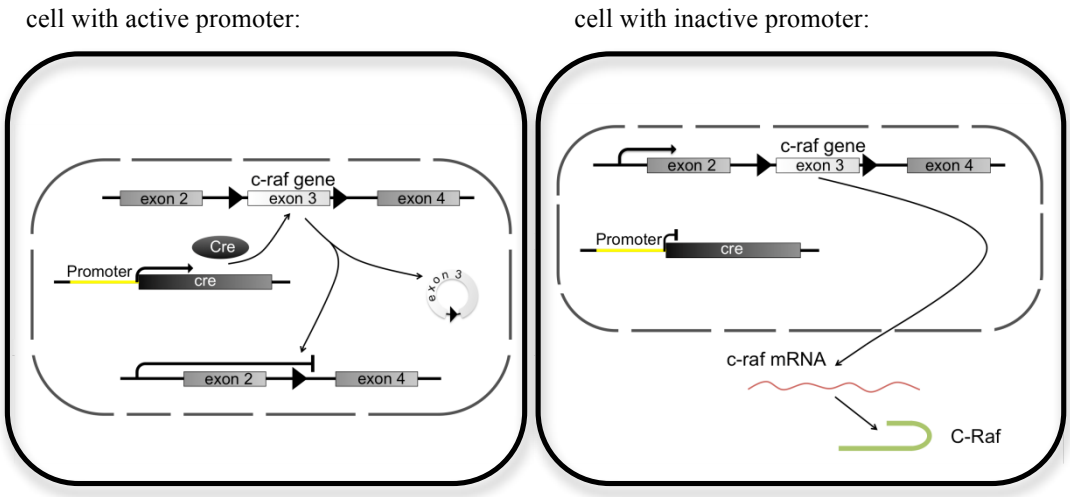

Figure 6. The Cre-LoxP-system

Upon activation of a specific promoter (either tissue specific or inducible) Cre recombinase is expressed and excises DNA flanked by two LoxP sites (marked by a black triangle). Excision of *c-raf* exon 3 creates a tissue-restricted or temporally-restricted gene knock out.

III.8 Tumor Model

Chemically-induced carcinogenesis has been extensively used to study all kinds of cancer types in rodents. One important paradigm emerging from these data is that carcinogenesis comprises three stages: initiation, promotion and progression (Fig. 7). Every cancer is believed to start with a single hit predisposing a normal cell to a malign development. This first step is categorized as initiation and is linked with irreversible changes in the genome of the affected cell. Promotion, the second stage, is marked by growth stimuli induced by tumor promoters, which enhance proliferation of susceptible cells. Upon withdrawal of tumor promoters, proliferation can normalize and newly formed neoplasias may regress (most likely through apoptosis), making promotion a reversible process. The last stage, progression, is completely irreversible. Neoplasias and pre-neoplastic lesions transform into malignant lesions in which proliferation is entirely independent of promoting agents. The hallmarks of these lesions are uncontrolled growth, genomic instability, inva-

sion and metastasis (Oliveira et al. 2007). Although it represents an oversimplification, this three-staged model is widely accepted as a working model.

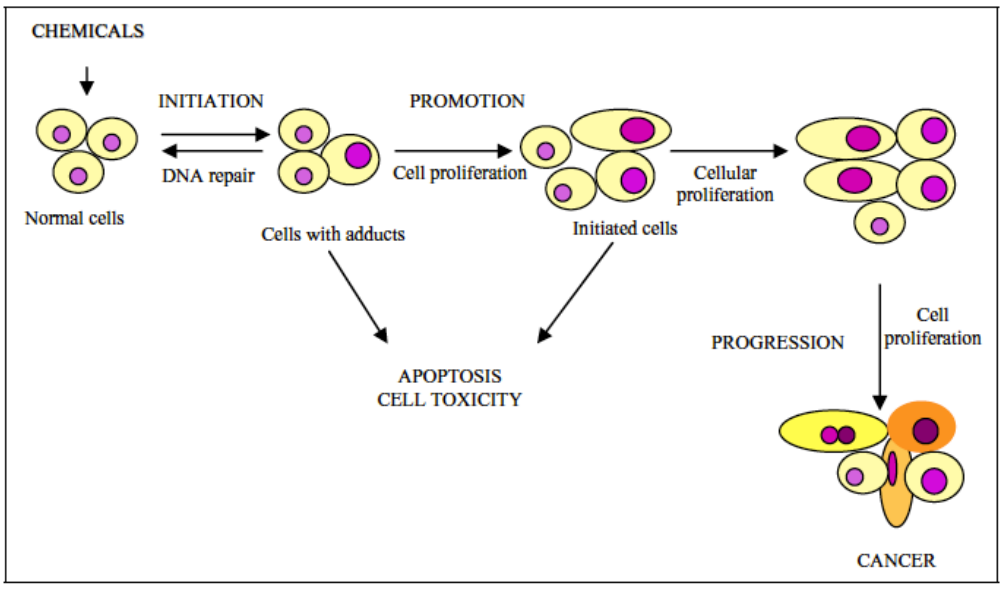

Figure 7. Three stage carcinogenesis model, adapted from (Oliveira et al. 2007)

Genotoxic chemical compounds initiate cells, which become malignant via promotion and progression and finally invade into neighboring tissue. It is important to note that promotion is a reversible step, whereas progression is irreversible.

N-Nitrosodiethylamine (NDEA) also called diethylnitrosamine or shortly DEN is frequently used to induce hepatocarcinogenesis in laboratory animals. DEN is classified as 'probable human carcinogen' by the International Agency for Research on Cancer review (IARC) and is found in tobacco smoke, meat and whiskey (Verna et al. 1996). Apart from inducing cancer in the liver of rodents, cancer development could also be detected in the skin, the respiratory tract, and the gastrointestinal tract (Park et al. 2009). Genetic analysis of gene expression patterns showed that in DEN-induced experimental tumors gene expression is similar to that of HCC patients with poorer survival rate, validating DEN-induced carcinogenesis as an accurate HCC model (Lee et al. 2004).

DEN itself is not excretable and needs to undergo biotransformation (Fig. 8) to unfold its genotoxic character (Verna et al. 1996). Biotransformation of DEN in

the liver involves CYP2E1, a member of the cytochrome P450 system (CYP). CYP2E1 initiates bioactivation of DEN via oxygen- and NADPH-dependent hydroxylation, leading to the production of α-hydroxyl-nitrosamine (Kang et al. 2007). This first activation step occurs mostly in pericentral hepatocytes, in which the enzymatic activity of CYP2E1 is highest. α-Hydroxyl-nitrosamine is further processed to an ethyl-diazonium ion (electrophilic) by cleavage of an acetaldehyde group. DNA damage results from the alkylation of nucleophilic DNA-bases by the electrophilic ethyl-diazonium ion (Heindryckx et al. 2009). In addition to its genotoxicity, DEN causes oxidative stress via the CYP system, which generates reactive oxygen species (ROS), further contributing to cancer development (Heindryckx et al. 2009).

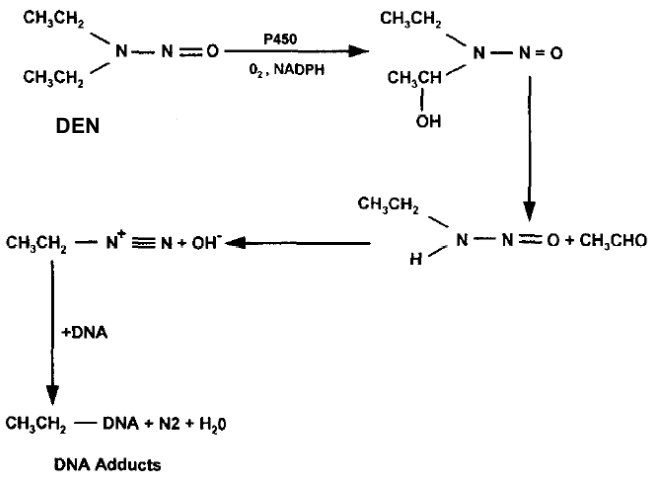

Figure 8. Biotransformation of DEN, adopted from (Verna et al. 1996)
DEN is hydroxylated by CYP2E1 to α-hydroxyl-nitrosamine and further processed to yield an ethyl-diazonium ion upon cleavage of acetaldehyde. The electrophilic ethyl-diazonium ion can alkylate DNA, thereby causing the formation of DNA adducts.

DEN-induce HCC development is not only dose-dependent but also age-, sex- and strain-dependent (Rao and Vesselinovitch 1973). Because of high hepatic proliferation rates in young animals, HCC develops much faster in these than in older ones (Vesselinovitch and Mihailovich 1983). Interestingly, HCC incidence upon DEN treatment differs drastically from males to females. Whereas 100% of DEN-treated male mice develop HCC, only 30% of treated females are affected (Nakatani et al. 2001). Considering that the lion's share of patients suffering from liver cancer is male, the pivotal question of gender-specific defense against carcinogens comes up. Estrogens were shown to have an inhibitory effect on HCC

development, thus rendering females less susceptible to HCC (Nakatani et al. 2001; Naugler et al. 2007). Further, strain-related differences in DEN-induced carcinogenesis were observed, originating from different methylation patterns dividing mouse strains into tumor sensitive and tumor insensitive strains (Buchmann et al. 1991).

DEN is often used in a combined two-step carcinogenesis system, in which a single application is followed by treatment with a promoting agent (e.g. Phenobarbital; Pb) administered over weeks or even months. The tumor-promoting characteristics of Pb have not been fully clarified, but they include the capability to influence the expression of CYP and enhancing oxidative stress (Waxman and Azaroff 1992; Watson and Goodman 2002; Imaoka et al. 2004). Pb treatment has been connected with alterations in proliferation through interaction with intracellular signaling networks and changes in the methylation of tumor suppressor genes (Heindryckx et al. 2009).

III.9 To Date: *c-raf* Deletion Promotes HCC Development and Progression in $c\text{-}raf^{\Delta hep/\Delta hep}$ Mice but not in $c\text{-}raf^{\Delta liv/\Delta liv}$ Mice (unpublished data, Maurer et al.)

Since C-Raf has been shown to be frequently over-expressed in HCC, and Sorafenib, an *in vivo* c-raf inhibitor (amongst others), is currently the only successful therapeutic approach in liver cancer treatment, studies on C-Raf in liver cancer development are indispensible. We generated conditional *c-raf* knock out mice using the Cre-LoxP system (see above) and induced HCC by a two-step carcinogenesis protocol. A single DEN application (*i.p.*) was administered to four weeks-old male mice, followed four weeks later by a promotion period in which they were fed Pb-supplemented diet. Wild-type controls as well as *c-raf* knock out mice developed HCC within 26-30 weeks upon treatment.

The two Cre transgenic lines described above were used to achieve conditional *c-raf* ablation. DEN/Pb-treated *c-raf*$^{\Delta hep/\Delta hep}$ animals displayed a significant increase in liver/body weight ratio, tumor number and tumor occupied area, when compared to *c-raf* $^{F/F}$ control animals. These results contradicted the expectations raised by the analysis of C-Raf expression in human HCC, since the knock out of a protein found over-expressed in HCC would be predicted to reduce cancer development. Apparently, disturbance of the ERK pathway and/or the pathways influenced by the kinase-independent function of C-Raf renders the liver more sensitive to tumor formation. Furthermore, mitotic and apoptotic indexes were similar in tumor-bearing *c-raf*$^{\Delta hep/\Delta hep}$ and *c-raf* $^{F/F}$ livers, thus suggesting that C-Raf plays a role in early HCC development, most probably during initiation. Therefore, we chose to analyze the events taking place shortly after DEN application. The analysis of proliferation showed a delay in *c-raf*$^{\Delta hep/\Delta hep}$ compared to *c-raf* $^{F/F}$ livers, but no difference in apoptosis could be detected. In addition, DEN-induced STAT3 activation was prolonged and further lipid droplet accumulation was increased in *c-raf*$^{\Delta hep/\Delta hep}$ livers. In contrast, enhanced tumorigenesis could not be observed in *c-raf*$^{\Delta liv/\Delta liv}$ compared to *c-raf* $^{F/F}$ animals treated with Poly I:C 30 weeks after DEN/Pb treatment but *c-raf*$^{\Delta liv/\Delta liv}$ as well as *c-raf* $^{F/F}$ mice treated with Poly I:C displayed both in general more tumorigenesis when compared to *c-raf* $^{F/F}$ not treated with Poly I:C

At least two explanations can be put forward to interpret these findings: firstly, and most likely, the reason for the differences in *c-raf*$^{\Delta hep/\Delta hep}$ and *raf*$^{\Delta liv/\Delta liv}$ animals is determined by the cell types affected by the knock out (parenchymal cells only in *c-raf*$^{\Delta hep/\Delta hep}$; and parenchymal/non-parenchymal cells, particularly Kupffer cells, in *c-raf*$^{\Delta liv/\Delta liv}$ mice); and secondly, the difference may stem from the pro-inflammatory Poly I:C treatment used to ablate *c-raf* in *c-raf*$^{\Delta liv/\Delta liv}$. Distinguishing between these two possibilities is the aim of this thesis.

IV. Results

IV.1 Liver-restricted *c-raf* Ablation

Conventional knock out of *c-raf* results in embryonic lethality, which correlates with increased fetal liver apoptosis (Mikula et al., 2001). Therefore, the conditional knock out system Cre/loxP was used to generate liver-restricted gene ablation. *c-raf* ablation in liver was detected by conventional PCR, which illustrated the conversion of floxed alleles (^{F}) into deleted alleles ($_{\Delta}^{hep}$ and $_{\Delta}^{liv}$) of *c-raf* (Fig. 9 A). Further, immunoblotting was used to verify the absence of C-Raf protein in liver tissue (Fig. 9B).

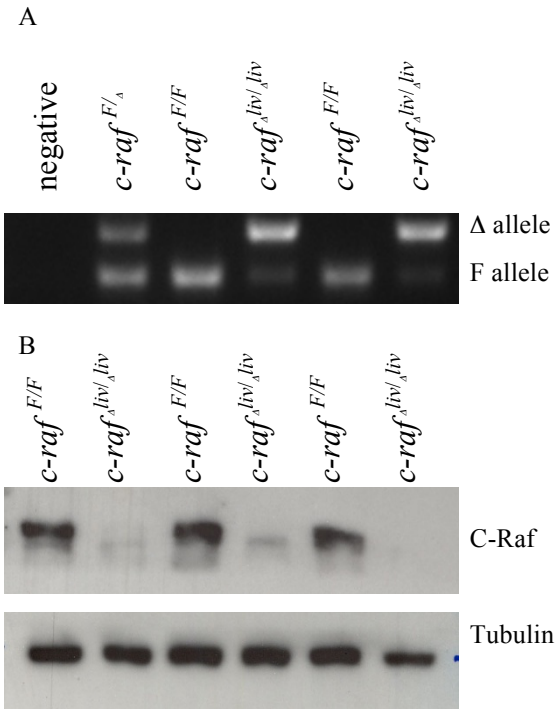

Figure 9. Liver Specific *c-raf* Ablation. A) PCR analysis: administration of Poly I:C triggers Cre expression, which in turn excises exon 3 of the floxed *c-raf* gene, resulting in the amplification of the Δ allele. A *c-raf* $^{F/\Delta}$ sample served as PCR control, to verify that both bands were amplified with a similar efficiency. B) Western blot for detection of C-Raf proteins in liver tissue. Deletion was efficient, since almost no C-Raf protein was detectable (residual protein may result from the inclusion of cells not affected by Poly I:C, e.g. endothelial cells).

Long-term effects of DEN treatment on *c-raf*$^{\Delta hep/\Delta hep}$ and *c-raf*$^{\Delta liv/\Delta liv}$ mice were analyzed by Maurer et al. (unpublished data). Increased susceptibility to tumor formation was found in *c-raf*$^{\Delta hep/\Delta hep}$ but not in *c-raf*$^{\Delta liv/\Delta liv}$ mice. The early effects after drug-induced liver injury in hepatocytes-restricted *c-raf* ablation compared to those of the simultaneous deletion in hepatocytes and non-parenchymal cells was central to this study. Maurer et al. further found accelerated liver cancer development in Poly I:C treated animals, which is needed for activation of Cre expression in *c-raf*$^{\Delta liv/\Delta liv}$ mice, suggesting a tumor promoting effect of this agent. In order to discriminate between the consequences of the different ablation patterns in *c-raf*$^{\Delta hep/\Delta hep}$ and *c-raf*$^{\Delta liv/\Delta liv}$ mice, and those of the Poly I:C administration in *c-raf*$^{\Delta liv/\Delta liv}$, we treated *c-raf*$^{\Delta hep/\Delta hep}$ animals with Poly I:C prior to DEN exposure and compared them directly to DEN-exposed *c-raf*$^{\Delta liv/\Delta liv}$ mice.

C-Raf, although not considered as the prime kinase actvating ERK, is in principle capable of driving this pathway. Therefore, *c-raf* ablation might negatively impinge on the levels of phosphorylated ERK. However, in Poly I:C-treated *c-raf* knock out mice (both *c-raf*$^{\Delta liv/\Delta liv}$ and *c-raf*$^{\Delta hep/\Delta hep}$) ERK activation was slightly elevated when compared to *c-raf* $^{F/F}$ littermates (Fig. 10 A-B). pERK levels equalized after DEN treatment in *c-raf*$^{\Delta liv/\Delta liv}$ compared to their Poly I:C treated wildtype controls (Fig. 10 A). By contrast, in livers of *c-raf*$^{\Delta hep/\Delta hep}$ mice ERK signaling reduced at 48h after DEN treatment when compared to their *c-raf* $^{F/F}$ littermates (Fig. 10 B).

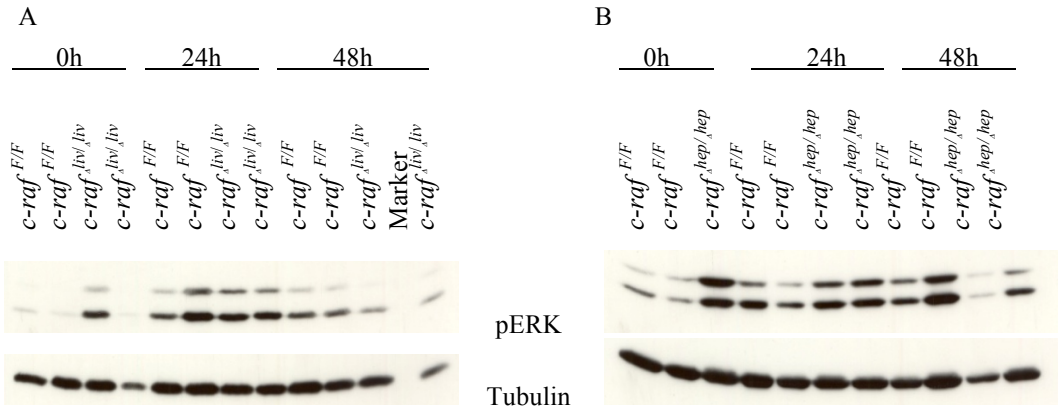

Figure 10. Western blot Analysis of ERK Activation in *c-raf* $^{F/F}$, *c-raf* $^{\Delta liv/\Delta liv}$ and *c-raf* $^{\Delta hep/\Delta hep}$ Mice treated with Poly I:C at 0h, 24h and 48h.

A) pERK immunoblot of liver lysates from Poly I:C injected *c-raf* $^{F/F}$ and *c-raf* $^{\Delta liv/\Delta liv}$ animals treated with DEN for 0h, 24h and 48h. B) pERK immunoblot of liver lysates from *c-raf* $^{F/F}$ and *c-raf* $^{\Delta hep/\Delta hep}$ animals treated with DEN for 0h, 24h and 48h. pERK levels are higher in untreated *c-raf* $^{\Delta liv/\Delta liv}$ and *c-raf* $^{\Delta hep/\Delta hep}$ animals treated with Poly I:C than in *c-raf* $^{F/F}$ or *c-raf* $^{F/F}$ littermates. This difference disappears upon DEN treatment (24h and 48h) in *c-raf* $^{\Delta liv/\Delta liv}$ mice (A). *c-raf* $^{\Delta hep/\Delta hep}$ animals showed a small reduction of ERK signaling 48h after DEN treatment (B).

Comparison of Liver Injury upon DEN treatment in Poly I:C-treated *c-raf* $^{F/F}$, *c-raf* $^{\Delta liv/\Delta liv}$ and *c-raf* $^{\Delta hep/\Delta hep}$ mice

DEN is a genotoxic agent, which induces damage and morphological changes in the liver. 24 hours after DEN application, macroscopic changes became visible as clear spots all over the liver of Poly I:C-treated *c-raf* $^{F/F}$ (Fig. 11 B), *c-raf* $^{\Delta liv/\Delta liv}$ and *c-raf* $^{\Delta hep/\Delta hep}$. These changes were reversible and regressed starting from 48 hours after DEN treatment as illustrated in Figure 11 C for *c-raf* $^{F/F}$ mice. Livers of Poly I:C-treated *c-raf* $^{F/F}$, c-*raf* $^{\Delta liv/\Delta liv}$, and *c-raf* $^{\Delta hep/\Delta hep}$ mice displayed similar DEN-induced macroscopic changes.

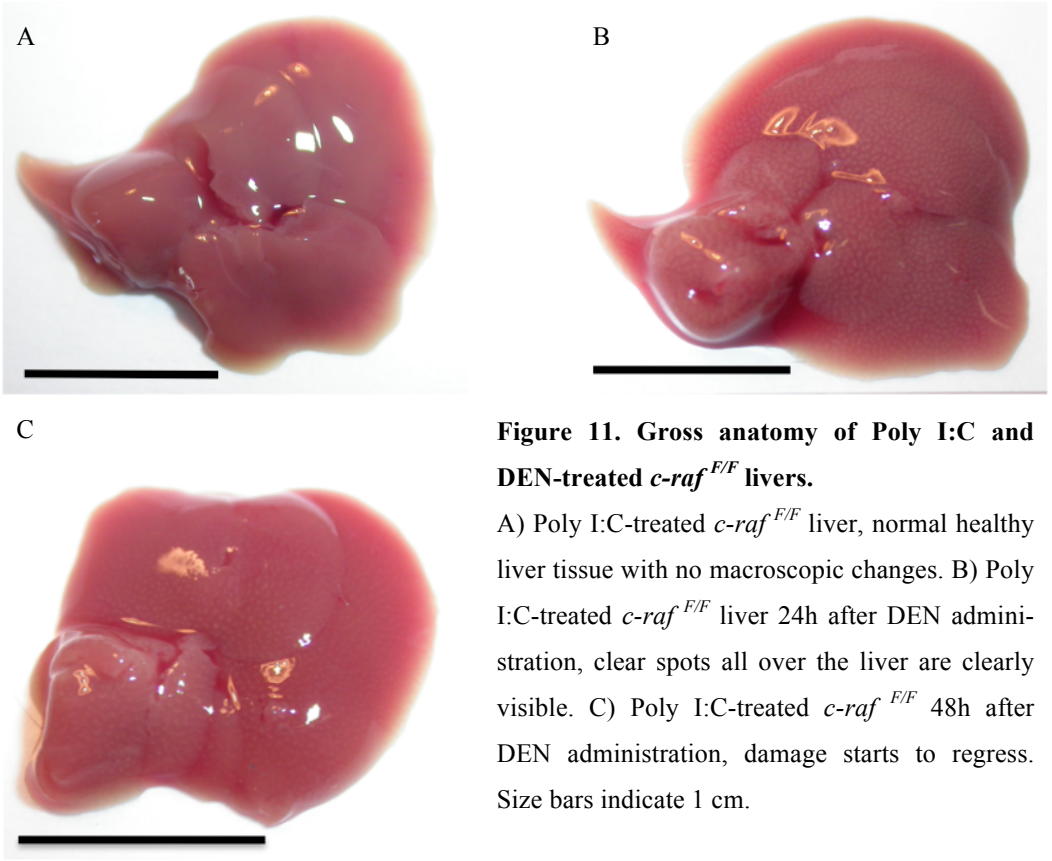

Figure 11. Gross anatomy of Poly I:C and DEN-treated *c-raf*$^{F/F}$ livers.

A) Poly I:C-treated *c-raf*$^{F/F}$ liver, normal healthy liver tissue with no macroscopic changes. B) Poly I:C-treated *c-raf*$^{F/F}$ liver 24h after DEN administration, clear spots all over the liver are clearly visible. C) Poly I:C-treated *c-raf*$^{F/F}$ 48h after DEN administration, damage starts to regress. Size bars indicate 1 cm.

Liver/body weight ratio is a parameter used to quantify changes in liver mass upon liver injury, in liver cancer and obesity studies, etc (Teoh et al. 2008; Bohm et al. 2010; Park et al. 2010). PolyI:C-treated *c-raf*$^{F/F}$ and *c-raf*$^{liv/\Delta liv}$ animals showed similar liver/body weight ratios, with values above 5% at 0h, 24h and 48h after DEN application (Fig. 12 A). Furthermore, no significant differences were observed between *c-raf*$^{F/F}$ and *c-raf*$^{hep/\Delta hep}$ at these time points (Maurer et al., unpublished data, not shown). PolyI:C-treated *c-raf*$^{F/F}$ and *c-raf*$^{hep/\Delta hep}$ littermates showed both lower liver/body weight ratios, with values around 4% (Fig. 12 B). The mice of this colony were usually 2 to 4 gram lighter than *c-raf*$^{F/F}$ and *c-raf*$^{liv/\Delta liv}$ animals of the same age and appeared more fragile. Further, *c-raf*$^{hep/\Delta hep}$ showed a tendency (not significant) towards a lower liver/body weight ratio (Maurer et al., unpublished data, not shown), possibly increasing after two Poly I:C injections, which are greatly challenging for these mice. The only significant difference between Poly I:C-treated *c-raf*$^{F/F}$ and *c-raf*$^{hep/\Delta hep}$ mice was observed 48h after DEN, a time point which might be affected by the delay in the proliferative response (see below).

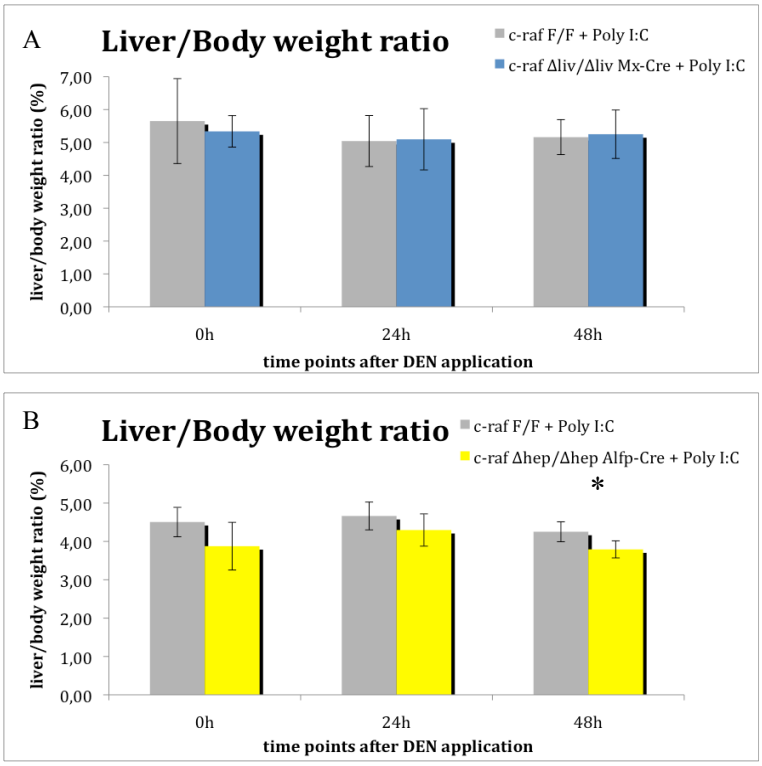

Figure 12. Liver/body weight ratio of poly I:C-treated *c-raf* $^{F/F}$, *c-raf*$^{liv/\Delta liv}$ and *c-raf*$^{hep/\Delta hep}$ Mice measured 0h, 24h and 48h after DEN injection.

A) Liver/body weight ratio of Poly I:C-treated *c-raf* $^{F/F}$ and *c-raf*$^{liv/\Delta}$ average between 5% and 6%, with no difference between knock out and wild type animals. Ratios are equal at time 0h and do not change within the observation period. B) The liver/body weight ratios of Poly I:C-treated *c-raf* $^{F/F}$ and *c-raf*$^{hep/\Delta hep}$ mice showed no significant difference at 0h and 24h. although the ratios were slightly lower in *c-raf*$^{hep/\Delta hep}$ animals. This decreased ratio became significant 48h after DEN treatment.

Hematoxylin and Eosin (H&E) staining of *c-raf*$^{hep/\Delta hep}$ livers revealed morphological changes around the central veins at 24h, in correspondence to the white spots observed macroscopically on livers after isolation. Hepatocytes in the pericentral area were bloated and showed a clear cell phenotype with translucent cytoplasm. These affected areas were lager in size in *c-raf*$^{hep/\Delta hep}$ mice when compared to *c-raf*$^{F/F}$ littermates (Maurer et al., unpublished data, not shown). This difference could not be observed when *c-raf*$^{liv/\Delta liv}$ mice were compared with their Poly I:C-treated *c-raf* $^{F/F}$ littermates at 24h (Fig. 13 C-D), and morphological

changes had (almost) disappeared at 48h in all genotypes (Fig. 13 E-F; and Maurer et al., unpublished data, not shown). A comparison of Poly I:C-treated *c-raf*$^{F/F}$ and *c-raf*$^{\Delta hep/\Delta hep}$ littermates showed larger affected areas in the knock out livers 24h after DEN treatment (Fig. 13 G-H), indicating that Poly I:C had neither a positive nor a negative effect on the increased DEN-induced liver damage observed by Maurer et al. in *c-raf*$^{\Delta hep/\Delta hep}$ livers.

The enlarged affected areas observed in *c-raf*$^{\Delta hep/\Delta hep}$ were postulated to be connected with enhanced susceptibility to tissue damage caused by DEN bioactivation around central veins. Liver injury and damage can be quantified via serum level measurement of two transaminases (aspartate aminotransferase – AST, and alanine aminotransferase – ALT). AST and ALT levels were determined for *c-raf*$^{\Delta hep/\Delta hep}$ and *c-raf* $^{F/F}$ littermates but showed no significant differences (Maurer et al., unpublished data, not shown), indicating that the origin of this difference lies somewhere else.

A second possible cause for the enlarged affected areas is increased lipid accumulation. DEN causes a disturbance in liver metabolism thereby inducing steatosis, which is an abnormal withholding of lipids in the liver and is known to be a predisposing factor in human HCC (Park et al. 2010). Staining of lipid droplets on frozen liver tissue sections with Oil Red O, a fat-soluble dye, showed enhanced steatosis in *c-raf*$^{\Delta hep/\Delta hep}$ compared to *c-raf* $^{F/F}$ livers 24h and 48h after DEN-treatment (Maurer et al., unpublished data, not shown). In contrast, DEN-induced lipid accumulation was similar in *c-raf*$^{\Delta liv/\Delta liv}$ and in their Poly I:C-treated *c-raf* $^{F/F}$ littermates at 0h, 24h and 48h (Fig. 14 A-F), Poly I:C-treated *c-raf*$^{\Delta hep/\Delta hep}$ animals displayed the same increased level of steatosis observed in *c-raf*$^{\Delta hep/\Delta hep}$ mice (Fig. 14 G-H), ruling out that Poly:C treatment reduced DEN-induced liver damage and lipid accumulation in *c-raf*$^{\Delta liv/\Delta liv}$ animals. The lack of these phenotypes in *c-raf*$^{\Delta liv/\Delta liv}$ livers is therefore likely due to the influence of non-parenchymal cells, particularly Kupffer cells, which are *c-raf* knock out in these organs, and may react differently to acute liver damage.

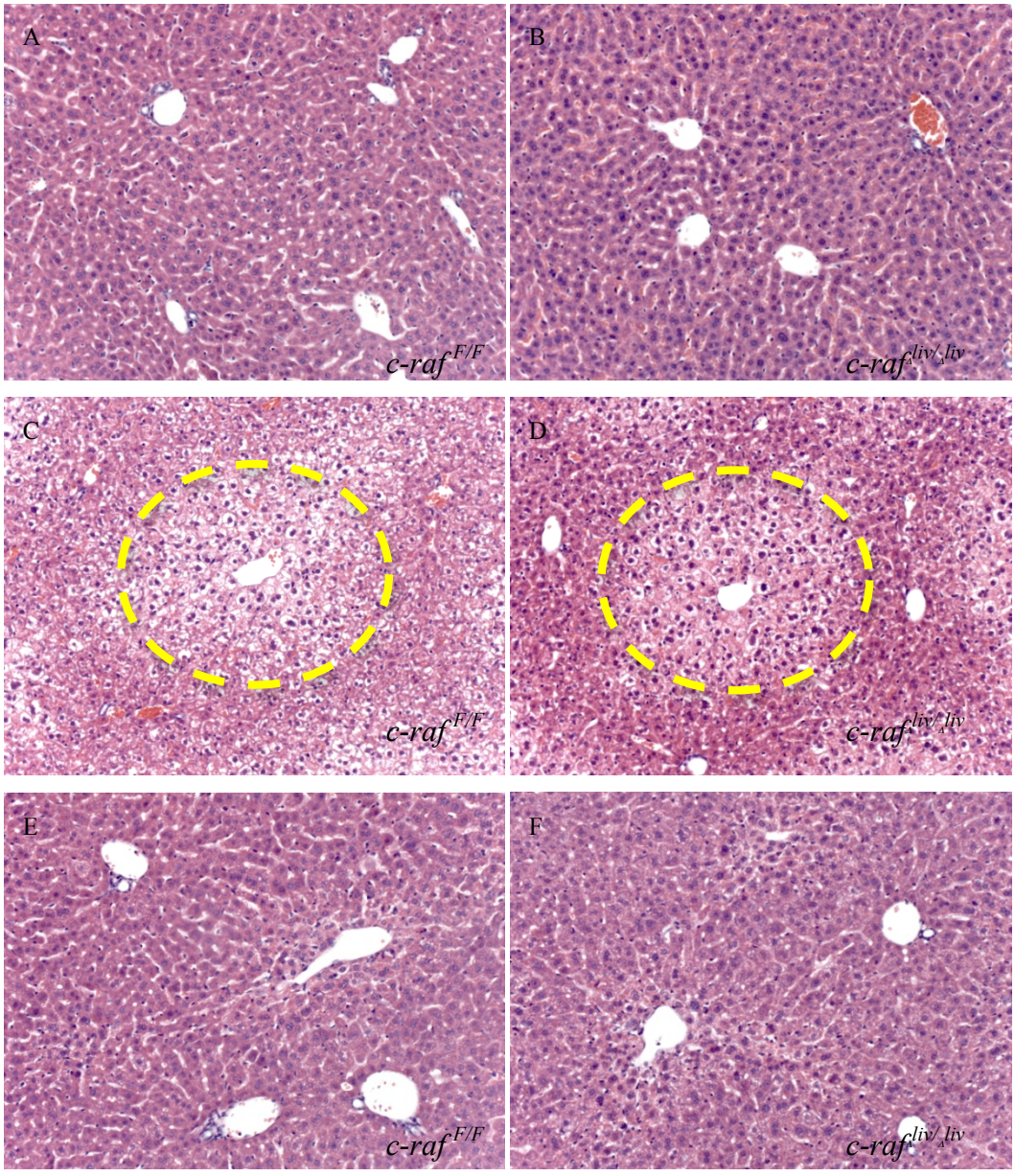
A
c-raf F/F
B
c-raf Δliv/Δliv
C
c-raf F/F
D
c-raf Δliv/Δliv
E
c-raf F/F
F
c-raf Δliv/Δliv

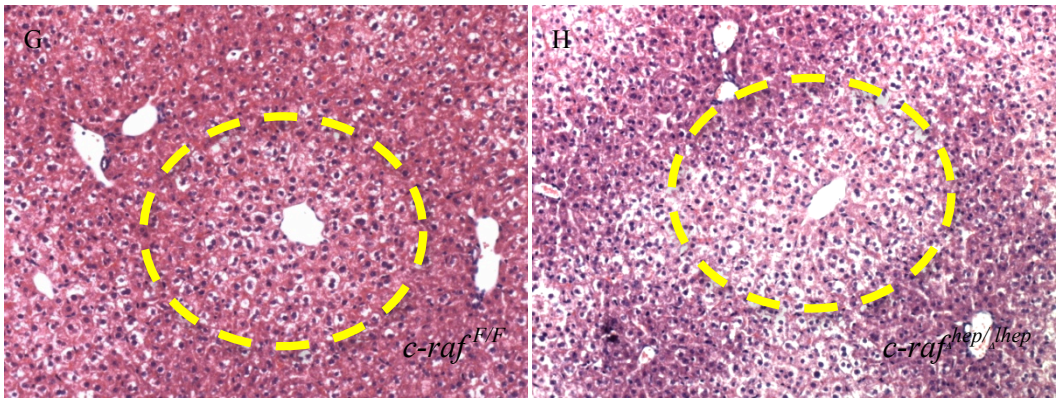

Figure 13. H&E Staining of Liver Sections from Poly I:C-treated *c-raf* $^{F/F}$, *c-raf*$^{liv/\Delta liv}$ and *c-raf*$^{hep/\Delta hep}$ Mice 0h, 24h and 48h after DEN-treatment.

A – B) Poly I:C treated *c-raf* $^{F/F}$ (A) and *c-raf*$^{liv/\Delta liv}$ (B), displaying healthy liver tissue. C –D). Poly I:C-treated *c-raf* $^{F/F}$ (C) and *c-raf*$^{liv/\Delta liv}$ (D) 24h after DEN, showing morphological changes around central veins including clear cell phenotype: the affected area, indicated by yellow circle has the same size in both genotypes. E – F) Poly I:C-treated *c-raf* $^{F/F}$ (E) and *c-raf*$^{liv/\Delta liv}$ (F) isolated 48h after DEN treatment, showing recovery from liver injury; the clear cell phenotype has disappeared and normal liver morphology is restored. G – H) Poly I:C-treated *c-raf* $^{F/F}$ (G) and *c-raf*$^{hep/\Delta hep}$ (H) 24h after DEN injection, showing morphological changes similar to those in (C) and (D); however, the affected area (indicated by yellow circles) is larger in *c-raf*$^{hep/\Delta hep}$ than in their littermate controls.

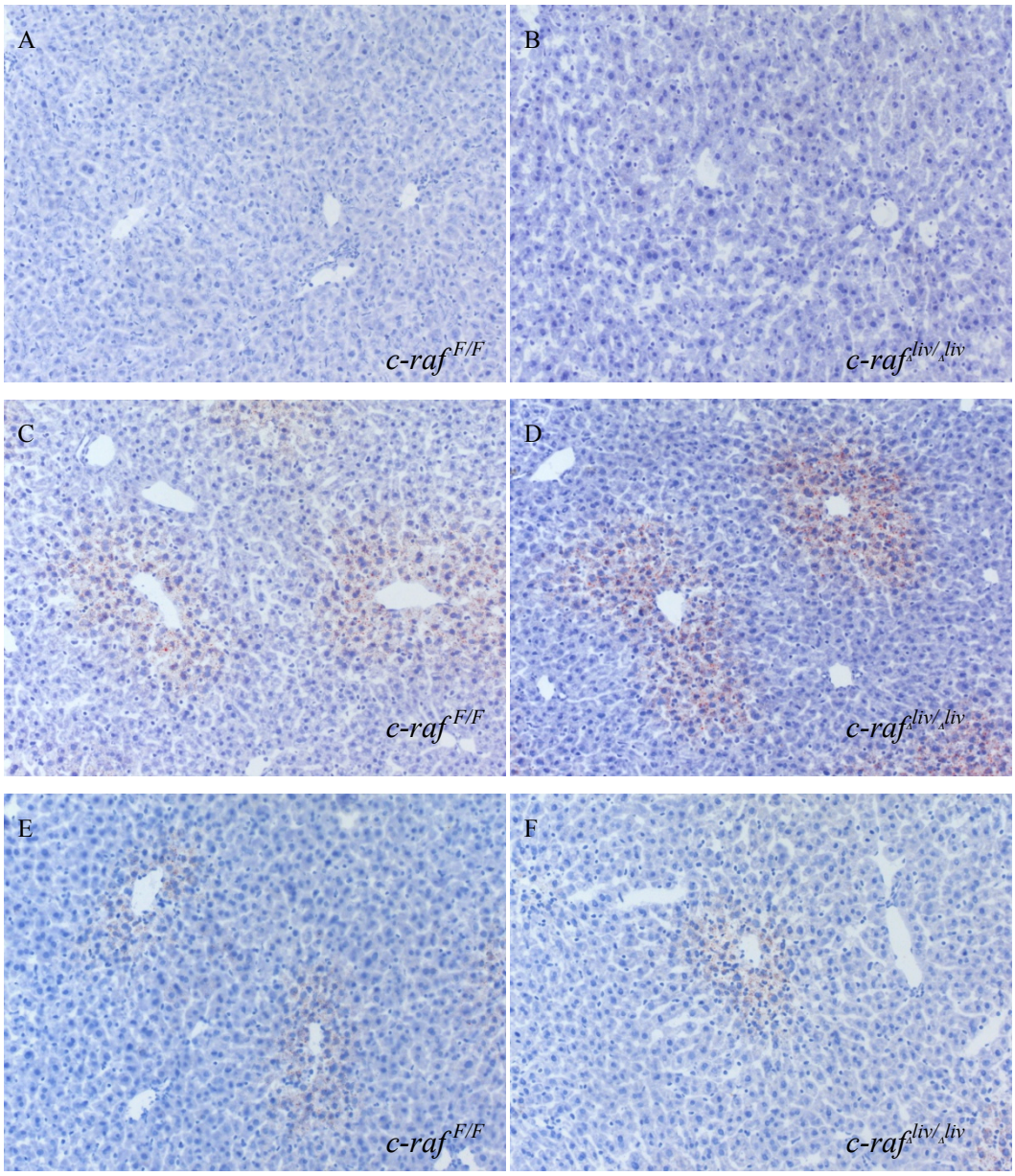
A
c-raf F/F
B
c-raf Δliv/Δliv
C
c-raf F/F
D
c-raf Δliv/Δliv
E
c-raf F/F
F
c-raf Δliv/Δliv

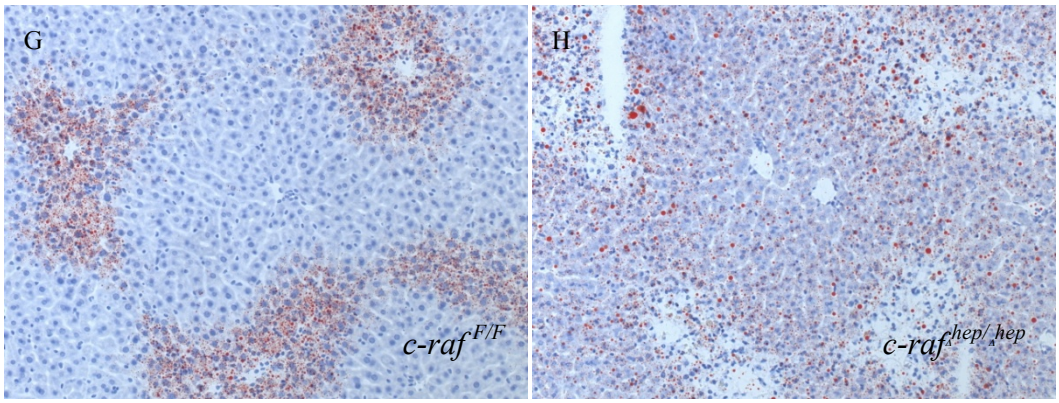

Figure 14. Oil Red O Staining of Frozen Liver Sections from Poly I:C-treated *c-raf* $^{F/F}$, *c-raf*$^{\Delta liv/\Delta liv}$ and *c-raf*$^{\Delta hep/\Delta hep}$ Mice 0h, 24h and 48h after DEN treatment.

A – B) Poly I:C-treated *c-raf* $^{F/F}$ (A) and *c-raf*$^{\Delta liv/\Delta liv}$ (B) display normal liver tissue. C – D). Poly I:C-treated *c-raf* $^{F/F}$ (C) and *c-raf*$^{\Delta liv/\Delta liv}$ (D) 24h after DEN treatment, showing lipid droplet accumulation around central veins, but no difference between the two genotypes. E – F) Poly I:C-treated *c-raf* $^{F/F}$ (E) and *c-raf*$^{\Delta liv/\Delta liv}$ (F) 48h after DEN treatment, showing normalization of the liver parenchyma. G – H) Poly I:C-treated *c-raf* $^{F/F}$ (G) and *c-raf*$^{\Delta hep/\Delta hepC}$ (H) 24h after DEN, displaying steatosis as in (C) and (D). In this case lipid droplet accumulation is more evident in *c-raf*$^{\Delta hep/\Delta hep}$ mice than in their littermates.

Cell death and apoptosis are tightly connected with tissue damage. DEN unfolds its cytotoxic property after bioactivation around the central veins, harming primarily surrounding cells. Most apoptotic cells could be in fact detected around the central veins by TUNEL (Terminal deoxynucleotidyl transferase dUTP nick end labeling) staining (Fig. 15 A). Statistical analysis did not show any significant difference between Poly I:C-treated *c-raf*$^{\Delta liv/\Delta liv}$ and *c-raf*$^{F/F}$ mice 0h, 24h and 48h after DEN (Fig. 15 B). Similar apoptotic indexes were also observed in *c-raf*$^{\Delta hep/\Delta hep}$ and their *c-raf* $^{F/F}$ littermates, untreated or treated with DEN for 24h and 48h (Maurer et al., unpublished data, not shown). Poly I:C-treated *c-raf*$^{\Delta liv/\Delta liv}$ and *c-raf* $^{F/F}$ displayed in general higher apoptotic indexes compared *c-raf*$^{\Delta hep/\Delta hep}$

and *c-raf* $^{F/F}$. This can be attributed to the Poly I:C application, since the *c-raf* $^{F/F}$ controls differ only in Poly I:C treatment and *c-raf*$^{hep/\Delta hep}$ and *c-raf*$^{liv/\Delta liv}$ animals are similar to their respective controls. This supports the hypothesis that Poly I:C may exert a 'priming' effect on the liver, leaving it in an post-inflammatory state, which allows a stronger and/or faster response to subsequent injury.

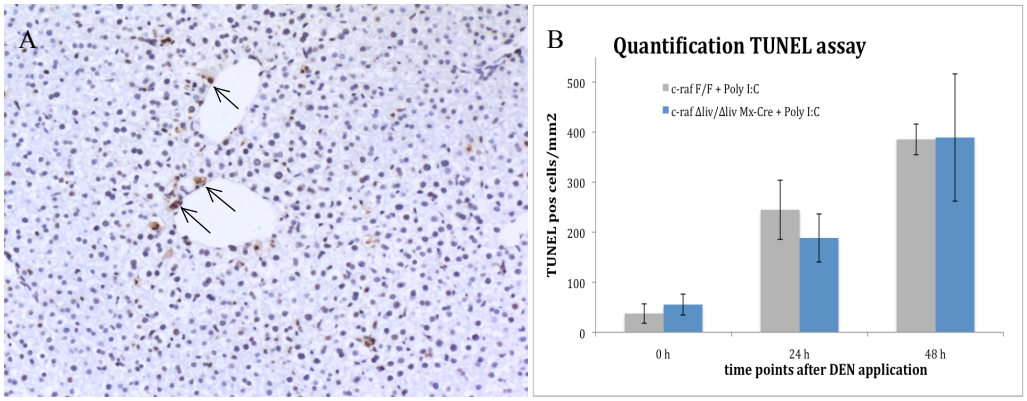

Figure 15. Apoptosis in Poly I:C and DEN-treated *c-raf* $^{F/F}$ and *c-raf*$^{liv/\Delta liv}$ Mice.

A) TUNEL staining of *c-raf*$^{liv/\Delta liv}$ liver tissue 24h after DEN treatment. Most apoptotic cells are observed around central veins, examples are indicated by black arrows. B) Statistical evaluation of TUNEL staining, showing no significant difference between Poly I:C-treated *c-raf*$^{liv/\Delta liv}$ and *c-raf* $^{F/F}$ mice.

IV.2 Inflammatory response of Poly I:C-treated *c-raf* $^{F/F}$, *c-raf*$^{liv/\Delta liv}$ and *c-raf*$^{hep/\Delta hep}$ mice to DEN treatment

As discussed in detail in the introduction, a cytokine-dependent (IL-6 and TNFα) and a growth factor dependent response (e.g. HGF) are activated upon liver injury to stimulate liver regeneration. The cytokine-dependent response mechanism involves activation of STAT3 via phosphorylation (pSTAT3).

STAT3 phosphorylation could be detected by immunohistochemistry in livers 24h and 48h after DEN application, and was much stronger in *c-raf*$^{hep/\Delta hep}$ mice than in *c-raf* $^{F/F}$ mice (Maurer et al., unpublished data, not shown). *c-raf*$^{liv/\Delta liv}$ mice showed inconsistent results, indicating in some cases stronger STAT3 activation, in some less and in others equal phosphorylation of STAT3 compared to Poly I:C-treated *c-raf* $^{F/F}$ controls (Fig. 16 C-D). In contrast, STAT3 phosphorylation in Poly I:C-treated *c-raf*$^{hep/\Delta hep}$ was elevated compared to Poly I:C-treated *c-raf* $^{F/F}$ control mice 24h (Fig. 16 G-H) but not 48h after DEN. This shift in the kinetics of pSTAT3 signaling compared to *c-raf*$^{hep/\Delta hep}$ mice probably depends on the Poly I:C injections, which are triggering an additional inflammatory response, thus driving this pathway shortly before DEN application (7 days), and leaving perhaps a post-inflammatory state behind. Upon DEN challenge, poly I:C *c-raf*$^{hep/\Delta hep}$ livers might react faster but also ease quicker than their controls, re-setting STAT3 activation back to *c-raf* $^{F/F}$ levels.

Western blot analysis confirmed elevated levels of pSTAT3 in Poly I:C-treated *c-raf*$^{hep/\Delta hep}$ compared to Poly I:C-treated *c-raf* $^{F/F}$ littermates 24h after DEN (Fig. 17). *c-raf*$^{liv/\Delta liv}$ mice showed inconsistent data concerning STAT3 activation, reflecting the picture provided by immunohistochemistry.

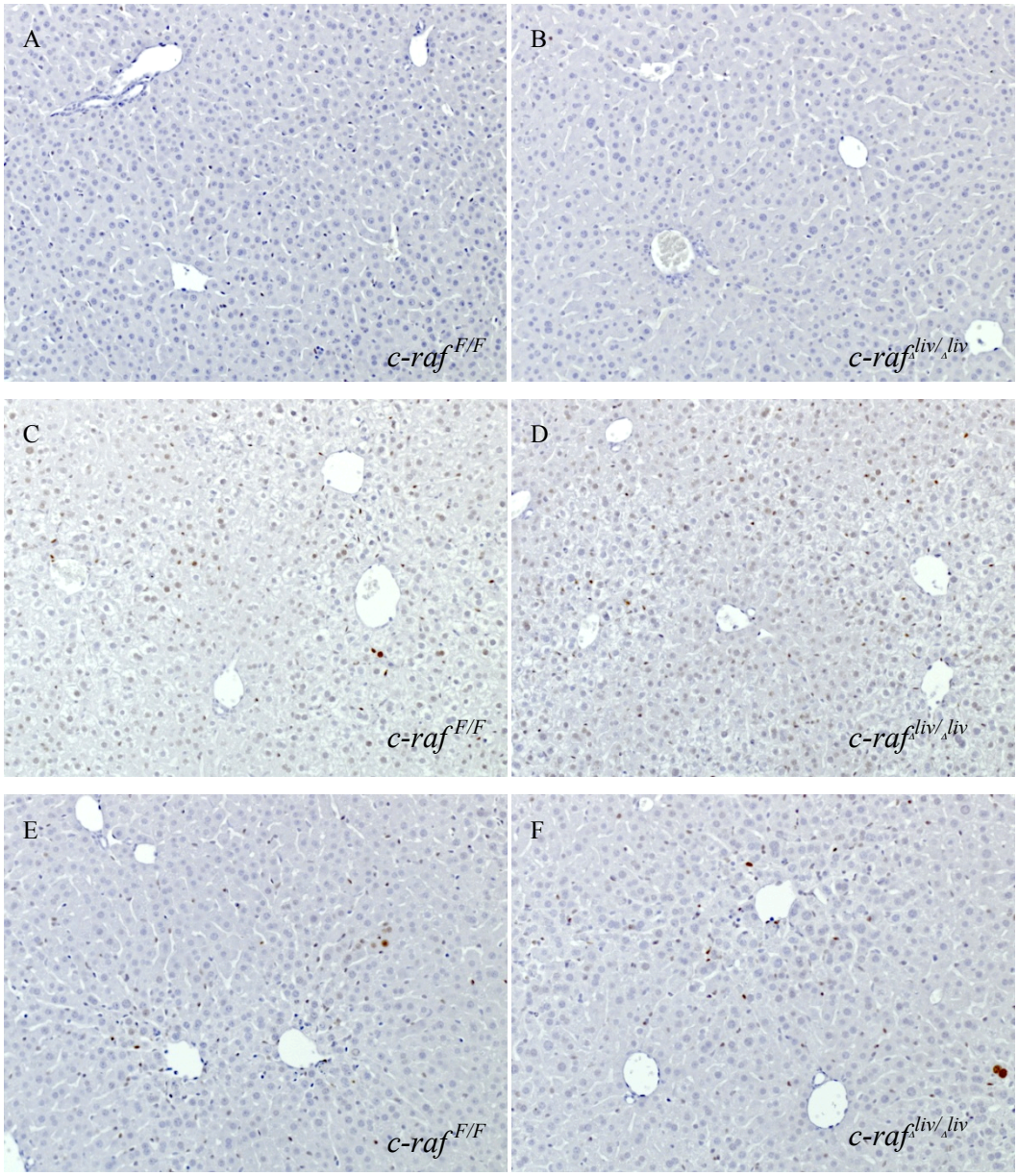
A
c-raf F/F
B
c-raf Δliv/Δliv
C
c-raf F/F
D
c-raf Δliv/Δliv
E
c-raf F/F
F
c-raf Δliv/Δliv

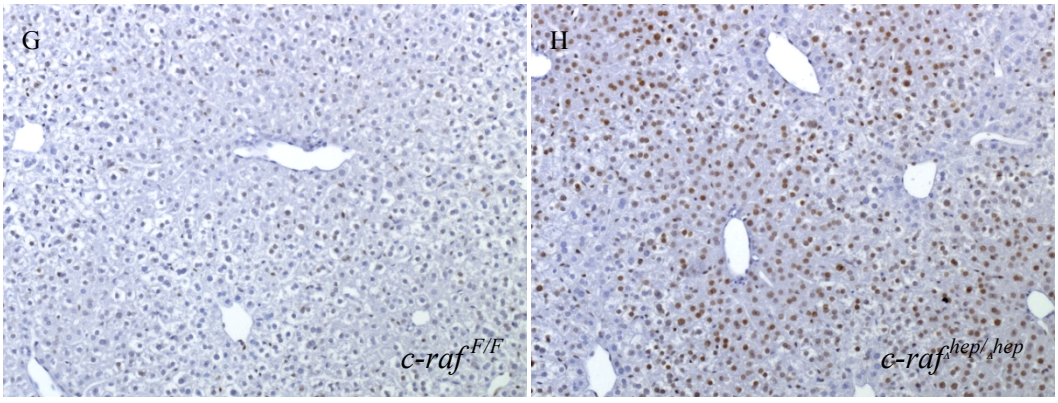

Figure 16. Immunohistochemistry of STAT3 Activation in Poly I:C-treated *c-raf* $^{F/F}$, *c-raf*$^{liv/\Delta liv}$ and *c-raf*$^{hep/\Delta hep}$ livers after DEN treatment.

A – B) Poly I:C-treated *c-raf* $^{F/F}$ (A) and *c-raf*$^{liv/\Delta liv}$ (B). STAT3 activation in liver tissue is undetectable. C –D). Poly I:C-treated *c-raf* $^{F/F}$ (C) and *c-raf*$^{liv/\Delta liv}$ (D) 24h after DEN, showing some STAT3 activation throughout the tissue, but no difference between *c-raf*$^{liv/\Delta liv}$ and control organs. E – F) Poly I:C-treated *c-raf* $^{F/F}$ (E) and *c-raf*$^{liv/\Delta liv}$ (F) livers 48h after DEN treatment, showing decreased STAT 3 activation, the majority of pSTAT3 positive cells being part of the non-parenchymal compartment. G – H) Poly I:C-treated *c-raf* $^{F/F}$ (G) and *c-raf*$^{hep/\Delta hep}$ (H) 24h after DEN treatment, showing much higher STAT3 activation in Poly I:C treated *c-raf*$^{hep/\Delta hep}$ around portal veins.

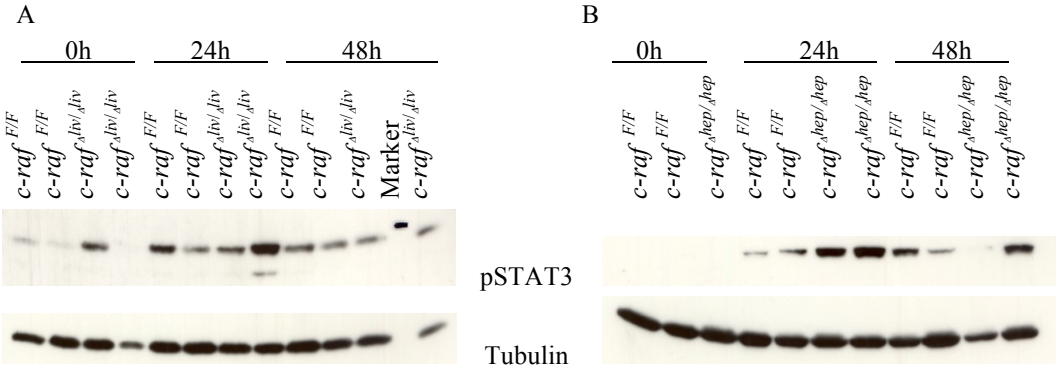

Figure 17. Western blot Analysis of STAT3 Activation in Poly I:C-treated ***c-raf*** $^{F/F}$, ***c-raf***$^{liv/\Delta liv}$ **and *c-raf*$^{hep/\Delta hep}$ liver lysates.**

A) pSTAT3 immunoblot of Poly I:C-treated *c-raf* $^{F/F}$ and *c-raf*$^{liv/\Delta liv}$ liver lysates prepared 0h, 24h and 48h after DEN treatment. pSTAT3 levels correlate with those observed by immunohistochemistry and show no significant differences between *c-raf* $^{F/F}$ and *c-raf*$^{liv/\Delta liv}$ animals. B) pSTAT3 immunoblot of Poly I:C-treated *c-raf* $^{F/F}$ and *c-raf*$^{hep/\Delta hep}$ liver lysates prepared 0h, 24h and 48h after DEN treatment. Stronger STAT3 activation is observed in *c-raf*$^{hep/\Delta hep}$ compared to *c-raf* $^{F/F}$ littermates 24h after DEN, in good correlation with the immunohistochemistry.

IL-6 is one of the triggers activating STAT3 phosphorylation, and since pSTAT3 was elevated in *c-raf*$^{\Delta hep/\Delta hep}$ and Poly I:C-treated *c-raf*$^{\Delta hep/\Delta hep}$ compared to their *c-raf* $^{F/F}$ littermates, an elevation of IL-6 could likewise be expected. The amount of IL-6 was determined by ELISA in lysates from liver tissue and in blood serum of mice treated with DEN (Fig. 18 A-C). IL-6 levels in the liver lysates were unexpectedly low and did not show any significant differences between Poly I:C-treated *c-raf*$^{\Delta hep/\Delta hep}$ and *c-raf* $^{F/F}$, between *c-raf*$^{\Delta liv/\Delta liv}$ and *c-raf* $^{F/F}$, or between *c-raf*$^{\Delta liv/\Delta liv}$ and *c-raf*$^{\Delta hep/\Delta hep}$ mice . IL-6 levels were elevated in *c-raf*$^{\Delta hep/\Delta hep}$ compared to *c-raf*$^{F/F}$ livers 6 hours after DEN treatment, but this effect had disappeared by 24h (Maurer et al., unpublished data, not shown). This indicates that IL-6 is expressed very early upon liver injury and that 24h and 48h after DEN treatment might be already too late to catch a difference between Poly I:C-treated *c-raf*$^{\Delta liv/\Delta liv}$ and *c-raf*$^{\Delta hep/\Delta hep}$ animals.

Immunohistochemistry of Poly I:C-treated *c-raf*$^{\Delta liv/\Delta liv}$ and *c-raf* $^{F/F}$ liver sections confirmed the ELISA data, showing no difference in IL-6 expression 0h, 24h and 48h after DEN. Localization of IL-6 in Poly I:C-treated *c-raf*$^{\Delta liv/\Delta liv}$ and *c-raf* $^{F/F}$ livers changed with treatment from pericentral to spread all over the tissue and back to central veins (Fig 19 A-F). This was at variance with *c-raf*$^{\Delta hep/\Delta hep}$ livers, where IL-6 staining was diffused at 0h but concentrated around central veins 6h after DEN treatment (Maurer et al., unpublished data, not shown), possibly indicating a different production pattern in *c-raf*$^{\Delta hep/\Delta hep}$ and *c-raf*$^{\Delta liv/\Delta liv}$ livers. This is most likely due to the inflammatory state triggered by PolyI:C injections, since again the only difference between the *c-raf* $^{F/F}$ mice used as littermate controls is the Poly I:C treatment, and *c-raf*$^{\Delta liv/\Delta liv}$ as well as *c-raf*$^{\Delta hep/\Delta hep}$ animals behave similarly to their controls.

Serum IL-6 could only be detected in *c-raf*$^{\Delta liv/\Delta liv}$ mice 24h after DEN (Fig. 18 C). The levels were below detection in all other genotypes (Fig.18 C; and Maurer et al., unpublished data, not shown). This indicates a possible effect of non-parenchymal cells *c-raf* on systemic IL-6 expression.

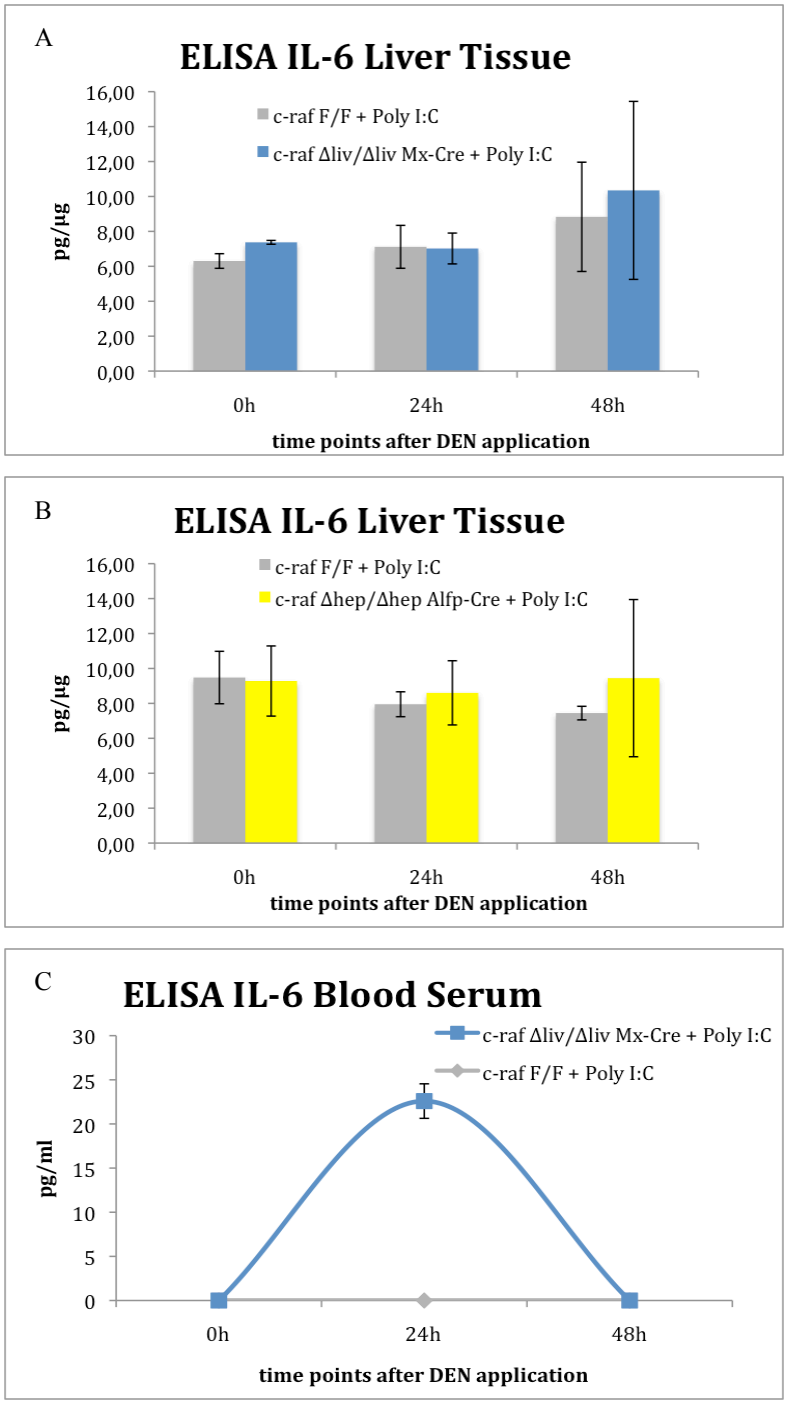

Figure 18. IL-6 ELISA from Poly I:C-treated *c-raf* $^{F/F}$, *c-raf*$^{liv/\Delta liv}$ and *c-raf*$^{hep/\Delta hep}$ liver and serum samples collected after DEN injection.

A) IL-6 levels in Poly I:C-treated *c-raf* $^{F/F}$, in *c-raf*$^{liv/\Delta liv}$ livers and B)in Poly I:C-treated *c-raf* $^{F/F}$ and *c-raf*$^{hep/\Delta hep}$ livers, which do not show any significant difference between the knock outs and littermate controls. C) IL-6 levels in blood serum of Poly I:C-treated *c-raf* $^{F/F}$ and *c-raf*$^{liv/\Delta liv}$ mice. IL-6 could be detected only in the serum of *c-raf*$^{liv/\Delta liv}$ treated with DEN for 24 hours.

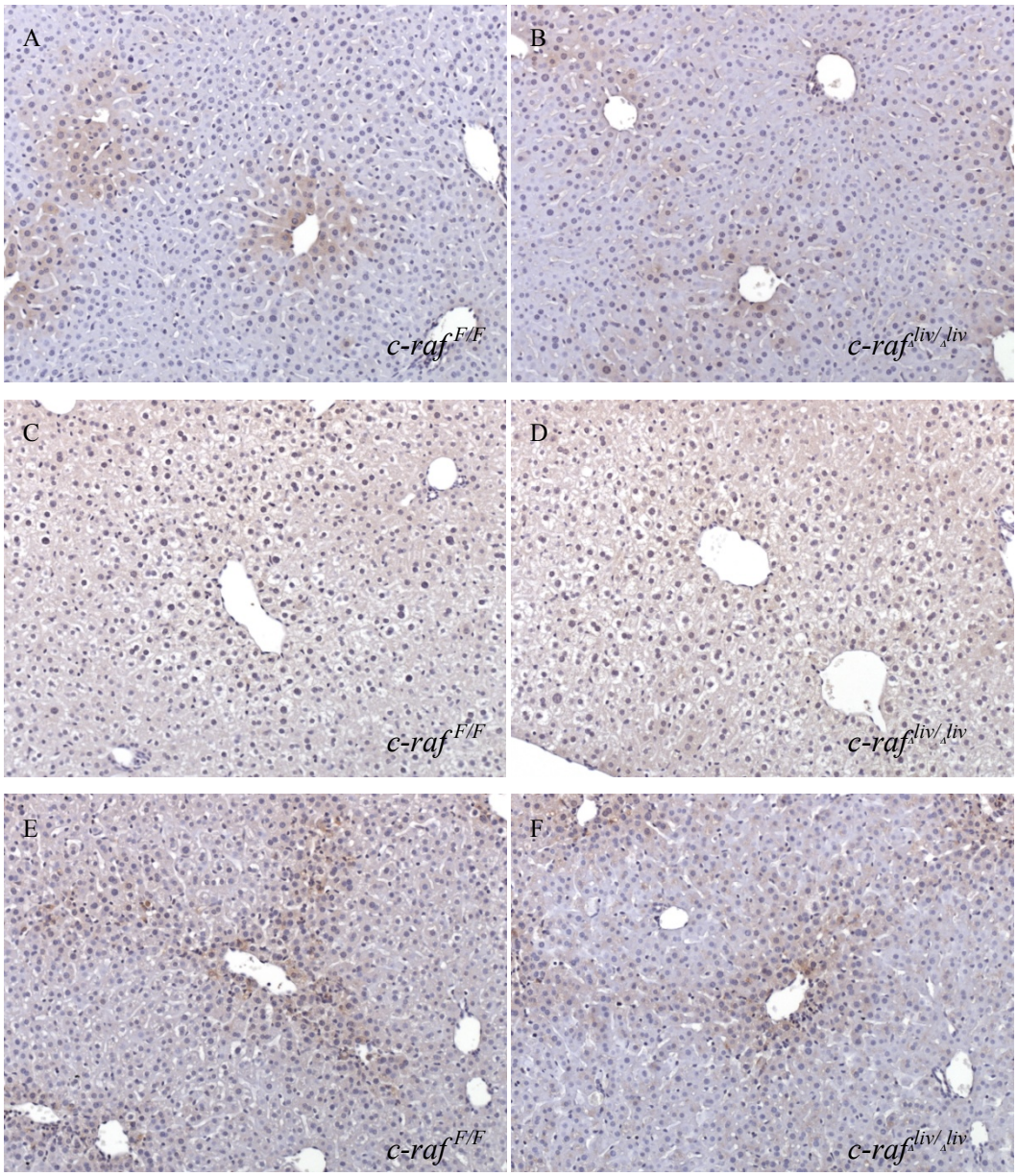

Figure 19. IL-6 Immunohistochemistry on Poly I:C-treated *c-raf* $^{F/F}$ and *c-raf*$^{\Delta liv/\Delta liv}$ liver sections isolated 0h, 24h and 48h after DEN injection.

A – B) Poly I:C-treated *c-raf* $^{F/F}$ (A) and *c-raf*$^{\Delta liv/\Delta liv}$ (B) livers with IL-6 expression around central veins. C –D). Poly I:C-treated *c-raf* $^{F/F}$ (C) and *c-raf*$^{\Delta liv/\Delta liv}$ (D) 24h after DEN treatment show diffused IL-6 staining throughout the tissue but no difference between *c-raf* $^{F/F}$ and *c-raf*$^{\Delta liv/\Delta liv}$ organs. E – F) Poly I:C-treated *c-raf* $^{F/F}$ (E) and *c-raf*$^{\Delta liv/\Delta liv}$ (F) 48h after DEN injection, showing IL-6 staining around the central veins.

IV.3 Post-DEN Regenerative Response in Poly I:C-treated *c-raf* $^{F/F}$, *c-raf* $^{\Delta liv/\Delta liv}$ and *c-raf* $^{\Delta hep/\Delta hep}$ Mice

The liver is an organ with a high regenerative capacity and reacts to injury with a proliferative response, thus replenishing the damaged cells which underwent apoptosis. In adult livers, proliferation is rarely observed except upon liver damage. In this study, the age of the animals was approximately one month and mice were not adult yet, which explains the proliferation observed in Poly I:C-treated *c-raf* $^{F/F}$ and *c-raf* $^{\Delta liv/\Delta liv}$ livers prior to DEN treatment (Fig. 20 B). Proliferation drops upon DEN-mediated injury (24h) and a proliferative response starts at 48h in Poly I:C-treated *c-raf* $^{F/F}$ and *c-raf* $^{\Delta liv/\Delta liv}$ littermates (Fig. 20 B). Maurer et al. observed a delayed proliferation in DEN-treated *c-raf* $^{\Delta hep/\Delta hep}$ livers compared to *c-raf* $^{F/F}$ littermates at 48h, with a peak at 72h (unpublished data, not shown). Poly I:C-treated *c-raf* $^{\Delta hep/\Delta hep}$ mice also displayed this proliferative delay (Fig. 20 C), while *c-raf* $^{\Delta liv/\Delta liv}$ did not lag behind in proliferation at 24h and 48h when compared to Poly I:C-treated *c-raf* $^{F/F}$ littermates (Fig. 20 B). This indicates that Poly I:C did not influence this parameter, which is therefore a 'real' discriminator between *c-raf* ablation in hepatocytes and parenchymal/non-parenchymal cells. Proliferating cells were mainly observed in the periportal region (Fig. 20 A). These cells are believed to replace the cells undergoing apoptosis in the pericentral region, which are most susceptible to liver injury due to the DEN metabolization pattern. Hepatocytes in *c-raf* $^{\Delta hep/\Delta hep}$ might be exposed to DEN for longer times or may accumulate more alterations in DNA compared to *c-raf* $^{\Delta liv/\Delta liv}$ or *c-raf* $^{F/F}$, since these animals are able to respond to the liver injury by replacing the damaged parenchyma faster than the *c-raf* $^{\Delta hep/\Delta hep}$ mice.

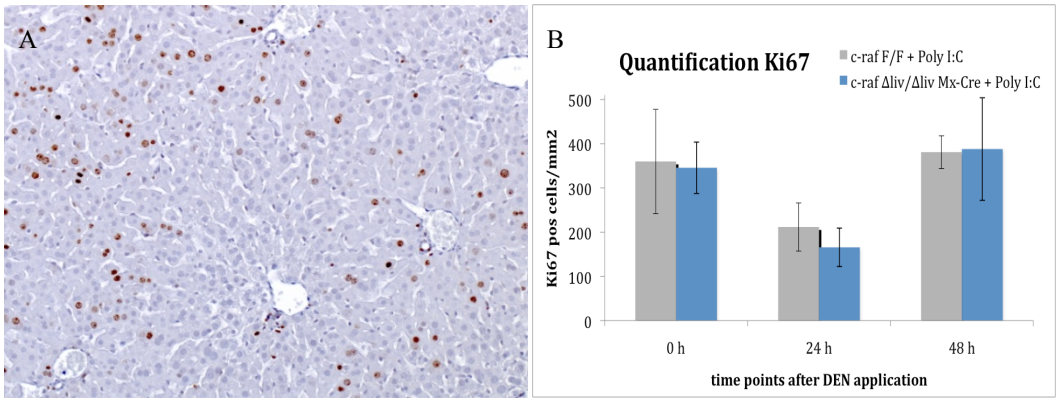

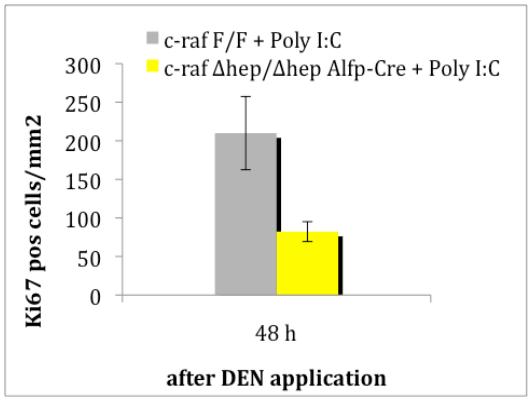

Figure 20. Ki67 staining and quantification of proliferation in Poly I:C-treated *c-raf* $^{F/F}$, *c-raf*$^{liv/\Delta liv}$ and *c-raf*$^{hep/\Delta hep}$ Livers after DEN treatment.

A) Ki67 staining of *c-raf*$^{liv/\Delta liv}$ liver tissue isolated 48h after DEN treatment. Most proliferating cells are observed around portal veins B) Statistical evaluation of Ki67 positive cells/mm^2 tissue, showing the same levels of proliferation in Poly I:C-treated *c-raf*$^{liv/\Delta liv}$ and *c-raf* $^{F/F}$ littermates. C) Statistical evaluation of Ki67 positive cells of Poly I:C-treated *c-raf*$^{hep/\Delta hep}$ and *c-raf* $^{F/F}$ littermates. *c-raf*$^{hep/\Delta hep}$ mice show a proliferation delay at 48h when compared to *c-raf* $^{F/F}$ controls.

IV.4 Analysis of systemic inflammatory changes in DEN-Treated Livers of Poly I:C-treated *c-raf* $^{F/F}$, *c-raf*$^{liv/\Delta liv}$ and *c-raf*$^{hep/\Delta hep}$ Mice

Analysis of blood samples (differential cell counts of lymphocytes, monocytes and granulocytes) showed no significant differences between Poly I:C-treated *c-raf* $^{F/F}$, *c-raf*$^{liv/\Delta liv}$ and *c-raf*$^{hep/\Delta hep}$ mice 0h, 24h and 48h after DEN. All values were in the physiological range (Fig. 21 A-C). *c-raf*$^{hep/\Delta hep}$ blood samples showed similar values and were also in the physiological range (Maurer et al., unpublished data, not shown). This indicates that DEN treatment does not elicit acute systemic inflammation and neither does Poly I:C, since no differences between Poly I:C-treated and untreated *c-raf* $^{F/F}$ were found (Maurer et al., unpublished data, not shown).

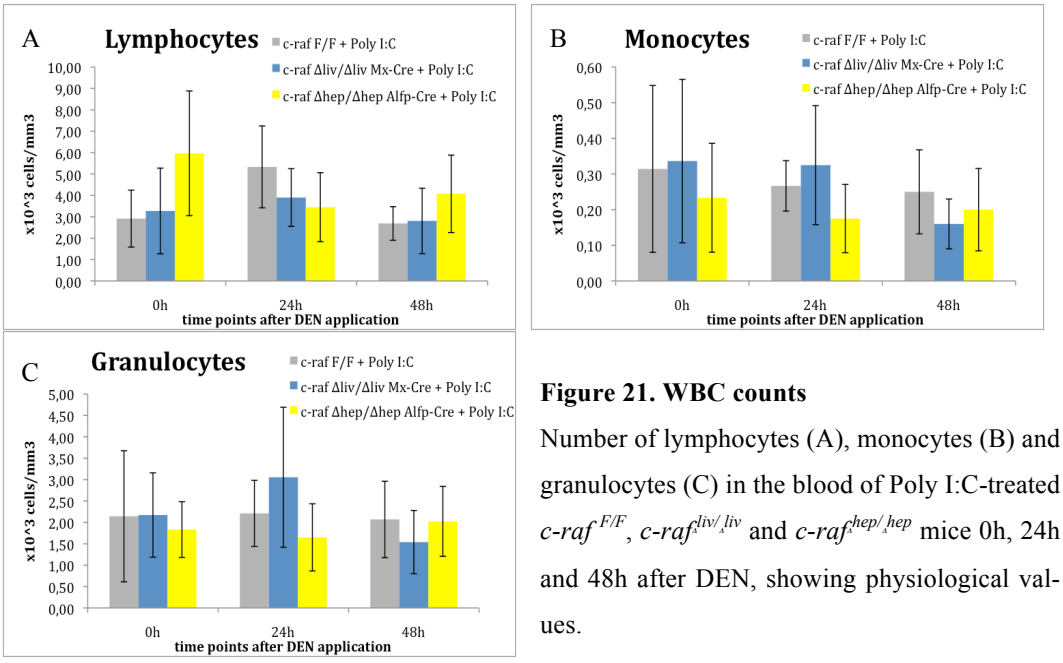

Figure 21. WBC counts

Number of lymphocytes (A), monocytes (B) and granulocytes (C) in the blood of Poly I:C-treated *c-raf* $^{F/F}$, *c-raf*$^{liv/\Delta liv}$ and *c-raf*$^{hep/\Delta hep}$ mice 0h, 24h and 48h after DEN, showing physiological values.

V. Discussion

The development of hepatocellular carcinoma is a complex and yet not fully understood process involving numerous changes in hepatocytes resulting in altered proliferation, differentiation, apoptosis and genomic instability (Farazi and DePinho 2006). The ERK signaling cascade has been frequently implicated in HCC development (Whittaker et al. 2010) and C-Raf overexpression has been consistently observed in these tumors (Hwang et al. 2004; Hopfner et al. 2008). Despite its established role in activating MEK and thereby driving the ERK pathway, C-Raf has distinct biological functions off this beaten track, including cross-talking abilities with Rho signaling (Ehrenreiter et al. 2005; Piazzolla et al. 2005; Ehrenreiter et al. 2009) and with the two pro-apoptotic kinases ASK1 (Chen et al. 2001; Yamaguchi et al. 2004) and MST2 (O'Neill et al. 2004; Matallanas et al. 2007). Interestingly, these pathways have been shown to participate in liver carcinogenesis (Zender et al. 2006; Hui et al. 2008; Wong et al. 2008), bringing C-Raf with its cross-talking nature into the focus of interest as a possible therapeutic target in HCC treatment.

Our results, so far, have revealed a surprising tumor suppressor function of C-Raf in chemically-induced hepatocarcinogenesis. Maurer et al. (unpublished data), could demonstrate enhanced tumor load and tumor multiplicity in mice with hepatocyte-restricted *c-raf* ablation (*c-raf*$^{\Delta hep/\Delta hep}$), which led to the hypothesis that *c-raf* suppressed tumor initiation. Concomitant deletion of *c-raf* in hepatocytes and hematopoietic-derived cells via the Mx-Cre system (*c-raf*$^{\Delta liv/\Delta liv}$) rescued the phenotype (Maurer et al., unpublished data). This might mean that C-Raf plays opposite roles in DEN-induced liver damage, depending on the cell type in which it is ablated. Alternatively, the Poly I:C treatment necessary for *c-raf* ablation in *c-raf*$^{\Delta liv/\Delta liv}$ mice may interfere with/neutralize the phenotype observed in *c-raf*$^{\Delta hep/\Delta hep}$ animals. In particular, Poly I:C treatment causes inflammation, which is a tumor promoter in this system. Indeed, Maurer et al. showed that DEN-induced HCC development is accelerated in *c-raf* $^{F/F}$ mice treated with Poly I:C compared to *c-raf* $^{F/F}$ animals (unpublished data), suggesting a tumor-promoting

effect of Poly I:C in DEN-induced liver carcinogenesis. This study was designed to distinguish between these two hypotheses. In order to discriminate which of the differences observed in HCC development in *c-raf*$^{liv/\Delta liv}$ versus *c-raf*$^{hep/\Delta hep}$ mice are based on the ablation in different tissues, and which are due to Poly I:C side effects, we compared *c-raf*$^{liv/\Delta liv}$ with *c-raf*$^{hep/\Delta hep}$ animals treated with Poly I:C.

DEN enters the liver via the portal vein, but becomes bioactivated around the central veins, by the cytochrome P450 system, which is expressed by the hepatocytes in this area (Kang et al. 2007). Consequently, most of the damage happens in this pericentral region. Increased apoptosis was not observed in *c-raf*$^{hep/\Delta hep}$ mice after DEN treatment. This was particularly puzzling, since C-Raf is known to be crucial for the survival of hepatoblasts during embryonic development (Mikula et al. 2001) and since it inhibits two pro-apoptotic kinases (Chen et al. 2001; O'Neill et al. 2004). However, four distinct consequences of hepatocyte-restricted *c-raf* ablation could be identified in DEN-treated mice: larger damaged areas around the central veins, increased steatosis, increased and prolonged STAT3 signaling, and a delay in the compensatory proliferative response (Maurer et al., unpublished data).

These phenotypes were not observed when *c-raf* was ablated in hepatocytes and non-parenchymal, hematopoietic cells. The area of damage, the degree of steatosis and STAT3 phosphorylation induced by DEN were similar in *c-raf*$^{liv/\Delta liv}$ mice and *c-raf* $^{F/F}$ littermates treated with Poly I:C. Furthermore, unlike the *c-raf*$^{hep/\Delta hep}$ animals, *c-raf*$^{liv/\Delta liv}$ mice did not show any delay in DEN-induced compensatory proliferation. The phenotypes observed in *c-raf*$^{hep/\Delta hep}$ mice could also be observed when these animals were injected with Poly I:C before DEN treatment; therefore, the different responses of *c-raf*$^{hep/\Delta hep}$ and *c-raf*$^{liv/\Delta liv}$ animals to DEN treatment are due to the distinct ablation patterns (hepatocyte-restricted ablation versus ablation in parenchymal and non-parenchymal cells).

The increased DEN-induced liver damage observed in *c-raf*$^{hep/\Delta hep}$ animals compared to their wild type controls is most likely associated with enhanced lipid droplet accumulation, since the damaged and steatotic areas overlapped remarka-

bly (Maurer et al., unpublished data). Steatosis is connected with liver injury and impaired regenerative response (Vetelainen et al. 2007) and could therefore negatively affect the replacement of damaged hepatocytes, causing an increase in the pool of initiated cells. In line with this, proliferation was impaired in *c-raf*$^{\Delta hep/\Delta hep}$ mice (Maurer et al., unpublished data). By contrast, *c-raf*$^{\Delta liv/\Delta liv}$ mice were able to mount a normal compensatory proliferative response upon DEN-induced liver injury, and therefore efficiently replaced damaged cells with undamaged ones. In addition, steatosis has been shown to drive low-grade inflammation and to induce the release of inflammatory cytokines and hormones such as IL-1, IL-6, TNF-α, adiponectin and leptin by the adipose tissue and Kupffer cells (Park et al. 2010; Toffanin et al. 2010). Furthermore, steatosis was linked to the production of reactive oxygen species (ROS), which induces persistent DNA damage and leads to genomic instability (Toffanin et al. 2010). ROS generation, a consequence of DEN metabolization and steatosis, (Maeda et al. 2005; Toffanin et al. 2010) was indeed increased in hepatocytes of DEN-treated *c-raf*$^{\Delta hep/\Delta hep}$ compared to *c-raf* $^{F/F}$ mice (Maurer et al., unpublished data). Persistent steatosis and ROS accumulation could sustain an inflammatory state and increase tumor development in *c-raf*$^{\Delta hep/\Delta hep}$ animals. This does not happen in *c-raf*$^{\Delta liv/\Delta liv}$ mice, which do not show any signs of steatosis or reduced compensatory proliferation.

Inflammation is crucial for HCC development in humans and mice (Lin and Karin 2007; Berasain et al. 2009). STAT3 activation, which is involved in the inflammatory response after DEN-induced liver injury and further triggers the regenerative response, was stronger and more prolonged in *c-raf*$^{\Delta hep/\Delta hep}$ compared to *c-raf* $^{F/F}$ mice. This phenotype was not observed in *c-raf*$^{\Delta liv/\Delta liv}$ animals, suggesting that non-parenchymal cells lacking *c-raf* are poor producers of STAT3 stimulating cytokines, or that pre-treatment with Poly I:C and the resulting cytokine production masked this phenotype. The latter hypothesis could be excluded since Poly I:C-treated and untreated *c-raf*$^{\Delta hep/\Delta hep}$ displayed a comparable increase in DEN-induced STAT3 activation.

In conclusion, steatosis, proliferation and STAT3 signaling could all be traced back to the different ablation pattern between *c-raf*$^{\Delta hep/\Delta hep}$ and *c-raf*$^{\Delta liv/\Delta liv}$ mice, excluding Poly I:C as an interfering factor in the *c-raf*$^{\Delta liv/\Delta liv}$ system. Therefore, the data are consistent with a requirement of C-Raf in non-parenchymal cells to sustain increased tumorigenesis in *c-raf*$^{\Delta hep/\Delta hep}$ mice.

Cytokines and growth factors produced by non-parenchymal cells, with Kupffer cells being a major source, will alter signaling pathways in hepatocytes. These pathways include the MAPK pathways ERK, JNK and p38, as well as the NF-κB pathway. Future studies will monitor the production of cytokines and growth factors associated with liver injury and regeneration (Fausto et al. 2006; Lin and Karin 2007) in *c-raf*$^{\Delta hep/\Delta hep}$ and *c-raf*$^{\Delta liv/\Delta liv}$ mice, and will compare this pattern with that obtained by stimulating Toll-like-receptors in cultured *c-raf* knockout hepatocytes. The data collected by monitoring IL-6 in our study suggest that cytokines are expressed and released very quickly, within hours after DEN treatment, and are back to basal values at 24h. Shorter time points after DEN administration (e.g. 4h, 6h and 8h) might yield a better picture of cytokine expression in the injured liver.

A final aspect to be considered is the possible effect of *c-raf* ablation on its two interacting pro-apoptotic kinases MST2 and ASK1. As detailed above, apoptosis was not altered in *c-raf*$^{\Delta hep/\Delta hep}$ and *c-raf*$^{\Delta liv/\Delta liv}$ compared to *c-raf* $^{F/F}$ and Poly I:C-treated *c-raf* $^{F/F}$ littermates; still the MST2 signaling cascade is a negative regulator of growth in general and of hepatocarcinogenesis in particular (Pan 2010) and ASK1 was described to be involved in stress response (Hattori et al. 2009). Thus, an investigation of these pathways is warranted.

Finally, Maurer et al. observed that Poly I:C, which is needed for the activation of the Mx-promoter in *c-raf*$^{\Delta liv/\Delta liv}$ mice, accelerates DEN-induced carcinogenesis. Poly I:C application triggers an inflammatory response, thereby activating and additionally recruiting inflammatory cells to the liver, priming this organ and leaving behind a post-inflammatory state. Upon DEN-induced liver damage, animals pre-treated with Poly I:C (*c-raf*$^{\Delta liv/\Delta liv}$ and *c-raf* $^{F/F}$ littermates treated with

Poly I:C) displayed increased apoptosis compared to Poly I:C untreated mice (*c-raf*$^{hep/\Delta hep}$ and *c-raf*$^{F/F}$ mice). Cell damage and cell death in the liver can initiate the release of activating factors, stimulating particularly cells of the immune system, like Kupffer cells, natural killer (NK) cells and NKT cells. These activated cells will produce pro-inflammatory cytokines such as TNF-α, Interferon (IFN)-γ and IL-1, thereby recruiting more inflammatory cells, driving liver injury further (Fig. 22) (Holt and Ju 2006). This sustained inflammatory environment could be causal for the increased carcinogenesis in PolyI:C treated livers.

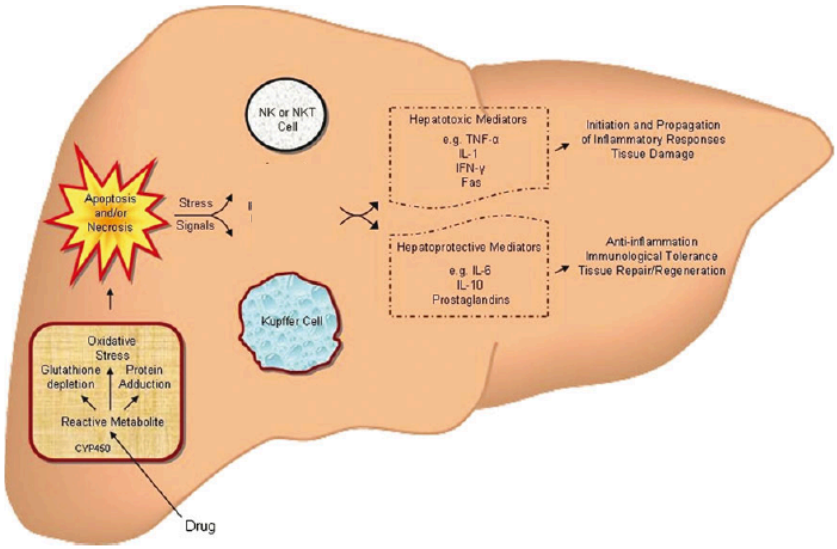

Figure 22. Drug-induced liver injury and its consequences, adapted from (Holt and Ju 2006) Proposed model of drug-induced liver damage, with non-parenchymal cells (Kupffer cells, NK and NKT cells) reacting to apoptotic signaling from surrounding cells, driving hepatoprotective and hepatotoxic pathways. The latter could be favored after Poly I:C treatment due to the post-inflammatory state left behind.

In a nutshell, the information provided by this study in comparison with the unpublished data from Maurer et al. indicates at least two cell type-dependent roles for C-Raf in liver tumorigenesis (Fig 23): a role as a suppressor of chemically-induced liver carcinogenesis in hepatocytes, and a tumor-promoting role in non-parenchymal cells. In non-parenchymal cells C-Raf might be involved in cytokine expression, initiating an inflammation state with elevated STAT3 signaling in

knock out hepatocytes. This tumor-promoting effect is lost with *c-raf* ablation in non-parenchymal cells. Elucidating in depth the interplay between *c-raf* knockout hepatocytes and non-parenchymal cells, especially Kupffer cells, will be beneficial for a better understanding and design of anti-cancer therapies, such as Sorafenib, targeting C-Raf among other molecules.

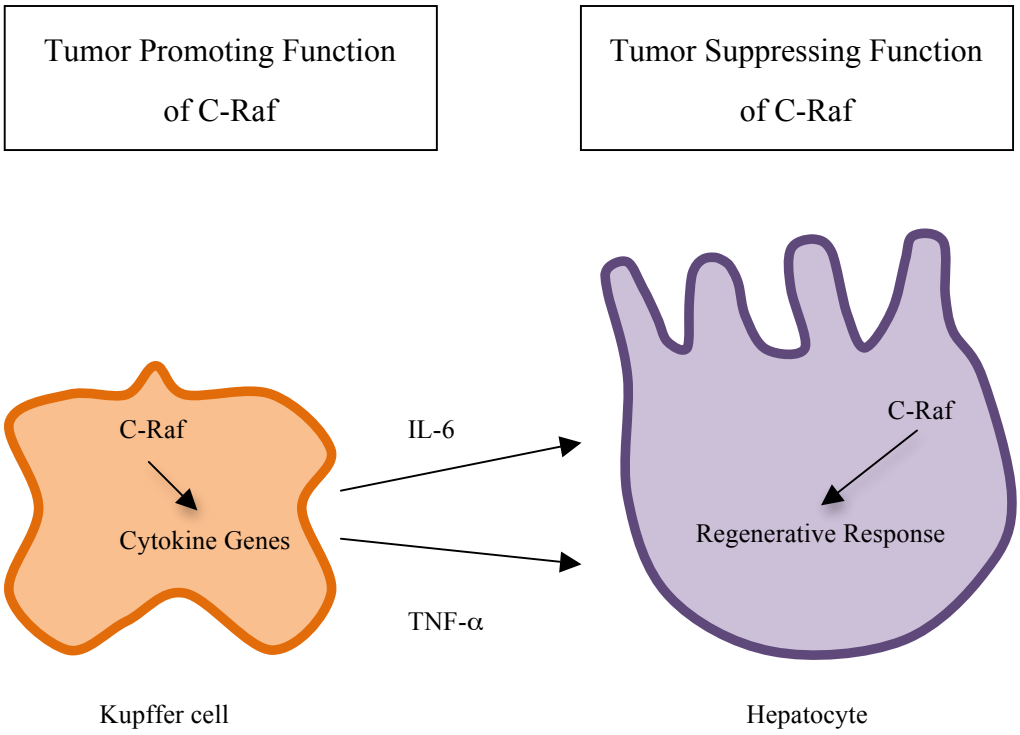

Figure 23. Hypothesis of C-Raf Function in Drug-induced Liver carcinogenesis

VI. Experimental Procedures

VI.1 Animals and Treatment

Animal Husbandry

All mice used in this study were kept on a SV 129/SVHsd pure background. Male inbred mice were maintained in filter top cages at ambient room temperature (RT 25°C), on autoclaved regular chow and autoclaved water, with a day/night cycle of 12h light and 12h dark under specific pathogen free (SPF) conditions, in the MFPL animal facility.

Generation of conditional *c-raf* ko mice

Mice (129/SVHsd) carrying loxP site flanked (floxed) exon 3 of the *c-raf* gene (*c-raf* $^{F/F}$) were crossed to transgenic mice, expressing the Cre recombinase under the control of the albumin promoter and α-fetoprotein enhancer (Alfp-Cre) (Kellendonk et al. 2000) or under the control of the Mx promoter (Mx-Cre) (Kuhn et al. 1995). Cre activity of Alfp-Cre transgenic mice was detected between day 9,5 post coitum (pc) and 10,5 pc (Kellendonk et al. 2000) thereby obtaining *c-raf*$^{\Delta hep/\Delta hep}$ animals. Mx-Cre mediated deletion of *c-raf* $^{F/F}$ was induced by two intraperitoneal (*i.p.)* injections of Poly (I:C) (Polyinosine-polycytidylic acid, Amersham Biosciences Ref. #27-4732-01**,** 100µg in 50µl PBS) on day 18 and 21 to obtain *c-raf*$^{\Delta liv/\Delta liv}$ mice . As control *c-raf* $^{F/F}$ littermates treated with Poly I:C were used.

c-raf$^{\Delta hep/\Delta hep}$ animals were analyzed by Maurer et al and were compared to *c-raf*$^{\Delta liv/\Delta liv}$ mice. As a control for possible Poly I:C effects *c-raf*$^{\Delta hep/\Delta hep}$ mice were treated with Poly I:C. Important to notice is that *c-raf*$^{\Delta hep/\Delta hep}$ have *c-raf* ablated in hepatocytes and need no Poly I:C for induction of Cre expression.

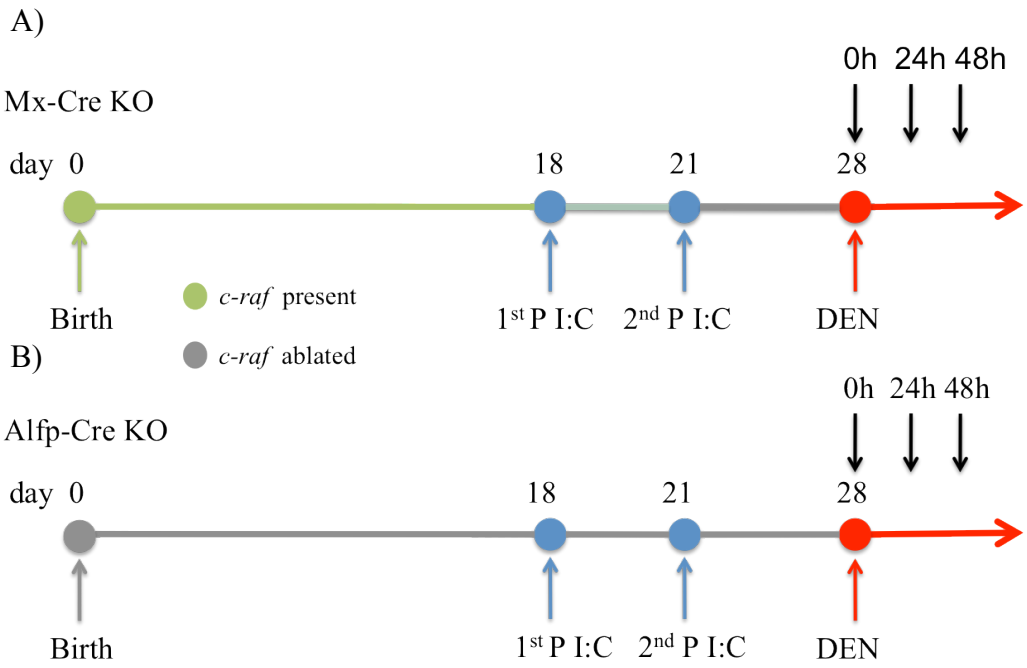

Figure 23. Conditional knock out and chemical induced carcinogenesis

A) Mx-Cre knock out model with two Poly I:C injections on day 18 and 21 to induce Cre expression and obtain *c-raf*$^{liv/liv}_{\Delta\Delta}$; B) Cre expression in Alfp-Cre mice is detected around pc10 and gene ablation of *c-raf* in hepatocytes is completed around birth. Poly I:C is administered only as a control and is not needed for the induction of Cre expression.

Administration of DEN

4-week-old *c-raf*$^{F/F}$, *c-raf*$^{hep/hep}_{\Delta\Delta}$ and *c-raf*$^{liv/liv}_{\Delta\Delta}$ male mice were injected *i.p.* with a single dose of DEN (Diethylnitrosamine, Sigma Ref. #N0258, 100mg/kg diluted in 0,9% NaCl, Sigma Ref. #S8776) (Fig. 23). Mice were killed by cervical dislocation and liver samples were collected before DEN injection (0h time point) and at indicated time points after DEN injection (24h and 48h).

VI.2 Blood Analysis

Blood (20 - 30 µL) was taken from tail vein and collected into EDTA coated MiniCollect tubes (Greiner Bio-One GmbH, Ref. #4500476). Whole blood analysis was performed using the V-Sight Vet Hematology Analyzer (A. Menarini Diagnostics). Blood for serum analysis was collected by cardiac puncture after killing mice with CO_2. Samples were left 30 min at RT for clotting and were centrifuged at 1.500 rounds per minute (rpm) for 10 min. Clear serum was collected, flash frozen in liquid nitrogen and stored at -80°C for further use.

VI.3 DNA Methods

Genomic DNA Preparation from Mouse Tissue

Tissue samples were digested in 90µL Viagen DirectPCR-Tail (Peqlab Ref. #31-102-T) + 10µL freshly added Proteinase K (10mg/mL, Sigma Ref. #P6556) o/n in a water bath at 55°C. After incubation, Proteinase K was inactivated by heating samples for 45 min at 85°C in a water bath.

Mouse liver tissue (~ 3-5 mm^3) was digested in 200µL tail buffer incl. 10% freshly added Proteinase K (10mg/mL, Sigma Ref. #P6556) o/n in a water bath at 55°C. On the next day, 100µL of saturated NaCl solution was added to the digested liver tissue, mixed and centrifuged at 13.000 rpm at 4°C for 10 min. 200µL of supernatant were transferred to a fresh tube and the pellet was discarded. DNA was precipitated by adding 150µL of isopropanol, inverted gently several times, then shortly vortexed and centrifuged at 13.000 rpm at 4°C for 5 min. Supernatant was discarded, the pellet was washed once with cold 70% EtOH and centrifuged at 13.000 rpm at 4°C for 5 min. EtOH was discarded, pellet was air dried for 10 min at 55°C on a thermo-mixer, dissolved in 50µL autoclaved water for 2 hours at 55°C and stored at 4°C. DNA concentration was measured with Nanodrop (ND-1000 Peqlab).

Tail buffer: 50mM Tris-HCl pH8, 100mM EDTA pH8, 100 mM NaCl

PCR Genotyping

Mouse toes and isolated livers were genotyped on a regular basis by polymerase-chain-reaction (PCR) and realtime PCR.

The *c-raf* genotype was analyzed by using the following PCR reaction mix:

Taq DNA Pol 2.0x Master Mix Red (Ampliqon, Ref.# 180306)	12,500 µl
Primer mpxr1 (100pM, VBC-Biotech)	0,125 µl
Primer mpxr2 (100pM, VBC-Biotech)	0,125 µl
Primer mpxr3D (100pM VBC-Biotech)	0,125 µl
ddH_20	9,630 µl
DNA	2,000 µl (≈ 200ng)
Final Volume	24,500 µl

c-raf primers

mpxr1, 5' TGT GCC CTT GGA ACC TCA GCA C-3'

mpxr2, 5'-ACA ACG AGA TAG ATG AGG AAA GCA-3'

mpxr3D, 5'CAC TGA AAT GAA AAC GTG AAG ACG-3'

PCR products: Primers mpxr1 and mpxr2 amplify a fragment of 280 base pairs (bp) when wt *c-raf* gene is present or 330 bp when *c-raf* gene is floxed; primers mpxr1 and mpxr3D amplify a fragment of 450 bp when *c-raf* gene is knocked out.

PCR was performed by GeneAmp® PCR System 9700 with the following cycling protocol:

	Initiation	98°C - 30sec
35 cycles	Denaturation	98°C - 10 sec
	Annealing	65°C - 30 sec
	Elongation	72°C - 45 sec
	Final Elongation	72°C - 1 min

The Cre recombinase transgene was detected by real-time PCR using the following Cre realtime PCR mix:

Fermentas 10x Taq Buffer with KCl	2,00 µl
Fermentas 25 mM MgCl2	3,60 µl
Fermentas dNTPs Mix 10mM each	0,50 µl
CRE US (100pM, VBC-Biotech)	0,08 µl
CRE DS (100pM, VBC-Biotech)	0,08 µl
Cre Probe (1:10)	0,25 µl
Fermentas Taq DNA Polymerase (5u/µL) (Ref.# EP0402)	0,20 µl
H_20	17,30 µl
DNA	2,00 µl
Final volume	26,00 µl

Real-time PCR was performed using an iCycler (Bio-Rad) with the following cycling protocol:

Initiation	94°C	5 min
Denaturation	94°C	15 sec
Annealing and Elongation	57°C	45 sec

Cre Primers
CRE US, 5'-ATT CTC CCA CCG TCA GTA CG-3'
CRE DS, 5'-GCA TTT CTG GGG ATT GCT TA-3'
CRE Probe, 5'-Fam-AAC CCT GAT CCT GGC AAT TTC GGC-BHQ1-3'
PCR Product: 95bp fragment

Agarose Gel Electrophoresis

c-raf PCR products were directly loaded on a 2% Agarose gel (Agarose, Biozyme Ref. #840004, dissolved in TAE-buffer) supplemented with Ethidium bromide (5µL/100mL). Electrophoresis was performed at 80-100 V for 30-50 min and the DNA was visualized under UV-light with Alpha-Imager (Alpha Innotech, Biozym).

VI.4 Histology

Liver Isolation, Tissue Fixation and Preparation of Paraffin embedded Tissue Sections

Livers were isolated, washed in cold PBS and dissected on ice. The large liver lobe was fixed in 4% Paraformaldehyde (PFA, Sigma, Ref. #P6148-1KG, diluted in PBS) overnight at 4°C. The next day the large liver lobe was transferred into 70% ethanol, placed into an embedding cassette (Engelbrecht, Ref. #17980r) and processed in the Shandon Excelsior (Thermo Electron Corporation): 7x 1h of increasing alcohol concentrations 70%-100%, 3x 1h Xylene and 3x 1h 20 min wax. Dehydrated tissue samples were embedded the following day in paraffin using an embedding center (Shandon Histocenter3 - Thermo Electron Corporation).
Paraffin blocks were pre-cooled (-12°C) and 5 µm sections were cut (Leica RM 2155) and transferred onto the surface of a 45°C warm water bath where the tissue could spread. Sections were transferred to Superfrost Plus slides (Gerhard Menzel GmbH Ref. #J1800AMNZ), dried at 45°C o/n and stored at RT until further use.

Hematoxylin-Eosin staining (H&E)

H&E staining was performed with the staining assistant machine ASS-1 (Pathisto) by using the following protocol:

1. Tissue Clear (Sanova, Ref. #SAK-1466) 10 min
2. Tissue Clear 10 min
3. 100% EtOH 5 min
4. 100% EtOH 5 min
5. 90% EtOH 2 min
6. 70% EtOH 2 min
7. H_2O 2 min
8. Hematoxylin (Sigma Ref. #HHS32-1L) 6 min
9. H_2O 1 min
10. 0,37% HCl/EtOH 5 sec
11. H_2O 10 min
12. 70% EtOH 30 sec
13. 80% EtOH 30 sec
14. Eosin (Sigma, Ref. #HT110132-1L) 2 sec
15. 90% EtOH 1 min
16. 90% EtOH 1 min
17. 100% EtOH 1 min
18. 100% EtOH 1 min
19. Tissue Clear 5 min
20. Tissue Clear 5 min

H&E-stained sections were placed in Xylene (Sanova, Ref. #MKB-3410-1/1) for 10 min and mounted with Entellan (Merck, Ref. #UN1866).

Immunohistochemistry – General Steps

Deparaffinization and Rehydration

The first step of each staining was to remove paraffin from the sections and to rehydrate the tissue:

2x 10 min Xylene
2x 10 min 100% EtOH
2x 90 min 90% EtOH

Slides were then transferred to ddH_2O before proceeding with the next step.

Blocking Endogenous Peroxidase Activity

Slides were incubated for 10 min in peroxidase blocking solution (50-80% MeOH, 1% H_2O_2) to avoid background signaling from endogenous peroxidases, washed 10x with H_2O and left 5 min in ddH_2O.

Epitope Retrieval

Depending on the antigen of interest different antigen retrieval methods where used to expose and preserve the desired epitopes:

- Citrate buffer – Slides were placed in 10mM Tri-sodium-citrate-dehydrate-buffer (Applichem, Ref. #2006753) pH 6 for 20-30 min at sub-boiling temperature and cooled down at RT for 20 min.
  Antigen retrieval: Ki67
- Proteinase K – Slides were incubated with Proteinase K (20µg/mL in 10mM Tris/HCl pH 7,4) for 15 min at 37°C.
  Antigen retrieval: TUNEL

- EDTA – Slides were incubated in 1mM Ethylenediaminetetraacetic acid solution (EDTA, Sigma Ref. #03680-1KG) pH 8 for 10-15 min at sub-boiling temperature.
  Antigen retrieval: pSTAT3
- Trypsin/EDTA – Slides were incubated in 0,05% Trypsin-EDTA (PAA, Ref. #L11-003) in PBS for 12 min at 37°C.
  Antigen retrieval: IL-6

Blocking Non-Specific Binding

Slides were washed once with PBS for 5 min, transferred onto Shandon Coverplate™ (Thermo Scientific Ref. #72110017) and placed into a Shandon Sequenza rack (Thermo Scientific). 120µL of blocking solution (1,5% - 5% normal goat serum (NGS) in PBS or TBS-T) was applied on each section and incubated for 30 min to 1h in order to reduce background signaling resulting from unspecific binding.

3.3'-Diaminobenzidine tretrahydrocholrid (DAB) reaction

Slides were washed 3x 5 min with PBS, transferred into a staining jar and incubated with DAB solution for 7-8 min at RT. Tissue samples turned brown and sections were washed once with PBS for 5 min.

DAB solution: 1 DAB tablet (Sigma Ref. #D5905-100TAB) in 50 ml 0,2M Tris/HCl pH 7,4 + 50µL H_2O_2 freshly added

Counterstaining

Sections were counterstained with filtered Hematoxylin (Sigma Ref. #HHS32-1L, diluted 1:10 in ddH_2O) for 15-30 sec and washed 10 min under running tab water and 5 min ddH_2O.

Dehydration

Sections were dehydrated by incubating the slides as following:

2x 10 min 90% EtOH
2x 10 min 100% EtOH
2x 10 min Xylene

Mounting

Slides were mounted with Entellan (Merck, Ref. #UN1866).

Ki67 staining (proliferation)

- Deparaffinization and Rehydration
- Blocking endogenous peroxidase activity
- Epitope retrieval: Citrate Buffer (25min, 97°C, cooling down for 20 min)
- Blocking non-specific binding (1,5% NGS, 30 min)
- Primary antibody – Ki67 polyclonal rabbit anti-mouse antibody (Novocastra Ref. #NCL-Ki67p), 1:1000 in PBS, 120µL/slide, o/n, 4°C.
- Secondary antibody – Envision+ System-HRP Labelled Polymer Anti-Rabbit (Dako, Ref. #K4003).

  Slides were washed 3x 5 min with PBS between primary and secondary antibody. 3 drops of secondary antibody were applied per slide and incubated for 30 min at RT.
- DAB reaction
- Counterstaining
- Dehydration
- Mounting

***In situ* cell death detection kit, POD (Roche, Ref. #11684817910) – TUNEL assay**

- Deparaffinization and Rehydration
- Blocking endogenous peroxidase blocking
- Epitope retrieval Proteinase K (15 min, 37°C)
- Positive control – selected section for positive control was treated 10 min with 25 units DNase diluted in DNase buffer (Fermentas Ref. #EN0521) at RT and washed once with PBS for 5 min
- Labelling – Sections were incubated with reaction mix (kit: 50µL from vial 1 and 450µL from vial 2) 50µL/slide for 1h at 37°C in a humidified chamber.
- Negative control – selected section for negative control was incubated with 50µL from vial 2 (kit) for 1h at 37°C in a humidified chamber.
- POD signal conversion – all sections were washed once with PBS for 5 min, incubated with POD converter (kit, 50µL/slide) for 30 min at 37°C in a humidified chamber and washed again once with PBS for 5 min
- DAB reaction
- Counterstaining
- Dehydration
- Mounting

pSTAT3 staining

- Deparaffinization and Rehydration
- Blocking: endogenous peroxidase activity
- Epitope retrieval EDTA (15min, 97°C)
- Blocking Non-specific binding (5% NGS in TBS-T, 30 min)
- Primary antibody – pSTAT3 (Tyr705) polyclonal rabbit antibody (Cell Signaling, Ref. #9145) 1:100 in 5% NGS in TBS-T, 120µL/slide, o/n, 4°C.
- Secondary antibody – Envision+ System-HRP Labelled Polymer Anti-Rabbit (Dako Ref. #K4003).

  Slides were washed 3x 5 min with TBS-T and 2x 5 min with PBS in between primary and secondary antibody. 3 drops of secondary antibody were applied per slide and incubated for 30 min at RT.
- DAB reaction

- Counterstaining
- Dehydration
- Mounting

IL-6 staining

- Deparaffinization/Rehydration
- Epitope retrieval: Trypsin-EDTA (12min, 37°C)
- Blocking: endogenous peroxidase activity
- Washing (2x 5 min TBS/0,0025% Triton X-100)
- Blocking: non-specific binding (5% NGS in TBS, 1h)
- Primary antibody – IL-6 polyclonal rabbit antibody (Abcam Ref. #ab6672) 1:200 in 1% BSA in TBS, 120µL/slide, o/n, 4°C.
- Secondary antibody – Envision+ System-HRP Labelled Polymer Anti-Rabbit (Dako Ref. #K4003).

  Slides were washed 3x 5 min with TBS-T and 2x 5 min with PBS between primary and secondary antibody. 3 drops of secondary antibody were applied per slide and incubated for 30 min at RT.
- DAB reaction
- Counterstaining
- Dehydration
- Mounting

Preparation of O.C.T embedded tissue sections

For cryo sections one smaller liver lobe was embedded into a Cryomold® (Sanova Ref. #4557) with O.C.T.™ compound (Sanova Ref. #4583) and flash frozen in liquid nitrogen. 7 µm thick sections were cut with a cryotome (Microm HM 500 OM), placed on Superfrost Plus slides (Gerhard Menzel GmbH Ref. #J1800AMNZ) and stored at -20°C.

Oil Red O staining (steatosis)

Sections were air dried for 30 min at RT and fixed with 4% PFA for 10 min, then washed once in ddH_2O for 5 min, incubated for 5 min in 60% isopropanol and incubated further for 10 min in a 0,3% Oil Red O solution (Sigma, Ref. #O0625). Samples were dipped shortly in 60% isopropanol and ddH_2O and counterstained with Hematoxylin, washed 10 min under running tap water and mounted with Glycerol (Merck, Ref. #ZC723095). Edges were sealed with commercially available nail polish.

VI.5 ELISA (Enzyme-linked immunosorbent assay)

ELISA was performed by using a kit from R&D system (DuoSet® ELISA Development System) and following the guidelines stated below:

Capture Antibody:	96-well plate was coated with 100µl/well diluted capture antibody o/n.
Blocking:	300µl/well blocking buffer was incubated for 2h.
Standard and Samples:	Serial dilution (1:2 – 1:32) of standard and serial dilution (1:100 – 1:3200) of 4 µg protein samples in Reagent Diluent were made, 100µL/well were applied and incubated for 2h.
Detection antibody:	100µl/well diluted biotinylated detection antibody was incubated for 2h.
Streptavidin-HRP:	100µl/well diluted Streptavidin-HRP solution was incubated for 20 min, protected from light.
Substrate Reaction:	100µl/well substrate solution was incubated for 25 min, protected from light. Enzymatic substrate reaction was stopped with 50µl/well Stop solution.
Results:	Absorbance was measured using a microtiter plate reader at 450nm. The concentration of cytokine in the samples was calculated according to a standard curve, taking into consideration only the values in the linear range.

All incubation steps were conducted at RT in a paraffin-sealed plate. Between steps, wells were washed three times with 400µL/well wash buffer (except before adding the stop solution).

Mouse IL-6 ELISA (R&D Systems, Ref. # DY406)

Capture antibody:	2µg/ml (diluted in PBS)
Standard:	1000pg/ml (diluted in Reagent Diluent)
Wash buffer:	0,05% Tween20 in PBS, pH 7,2 – 7,4
Blocking Buffer:	1% BSA in PBS, pH 7,2 – 7,4
Reagent Diluent:	1% BSA in PBS, pH 7,2 – 7,4
Streptavidin-HRP:	1:200 (diluted in Reagent Diluent)
Substrate Solution:	1:1 color reagent A (H_2O_2) and color reagent B (Tetramethylbenzidine)
Stop Solution:	2M H_2SO_4

VI.6 Protein Methods

Protein Lysates from Mouse Liver Tissue

Flash-frozen liver tissue samples (~20-40 mg) were mixed with 200-400µL ice-cold RIPA Buffer including freshly added inhibitors (~10µg tissue/µL RIPA Buffer) in a micro packaging vial (Peqlab, Ref. #91-PCS-TV) with 8 ceramic beads (Precellys-Kermaik-Kügelchen, 1,4 mm Peqlab, Ref. #91-PCS-CK14B). For tissue homogenization a Fast-Prep-24 machine (M.P. Biomedicals) was used: 2x 20 sec power 5. In between the two homogenization steps, samples were incubated for 2 min on ice. Lysates were centrifuged at 20.000g for 15 min at 4°C and the supernatants were transferred to a fresh tube, spun again at 20.000 g for 15 min at 4°C, supernatants transferred again to a fresh tube and immediately flash-frozen in liquid nitrogen. A small aliquot of the lysate was kept for protein concentration measurements (Bradford protein assay – see below).

RIPA Buffer: 50 mM Tris HCl pH 8, 150mM NaCL, 1% TX-100, 0,5% Sodium Deoxycolate (added with inhibitors), 0,1% SDS, stored at 4°C in dark.

Inhibitors (added freshly): 1mM PMSF, 2,5x Protease-Inhibitor Cocktail, 1mM Na_3VO_4, 100nM Okadaic acid

Protein Concentration and Sample preparation

Protein concentration of lysates was determined using the Bradford protein assay (Bio-Rad, Ref. #500-0006). Bradford solution was diluted 1:5 in ddH_2O and 1ml was poured in each plastic cuvette. 5µL of sample or standard were added and incubated for 5 min before the absorbance was measured at 595nm with a spectrophotometer (U-2800A Hitachi). All measurements were done in duplicates or triplicates to avoid pipetting mistakes and 5µl of RIPA buffer was used as blank.

Standard curve: Serial dilutions of BSA stock solution (100µg/µL) in RIPA buffer (3,6/2,9/2,3/1,65/1/0,5 µg/µl) were prepared and measured using the Bradford protein assay. 5µl of each standard dilution were incubated 5 min in 1mL of diluted Bradford solution before measurement. The standard curve was calculated on the basis of the absorption of each standard dilution.

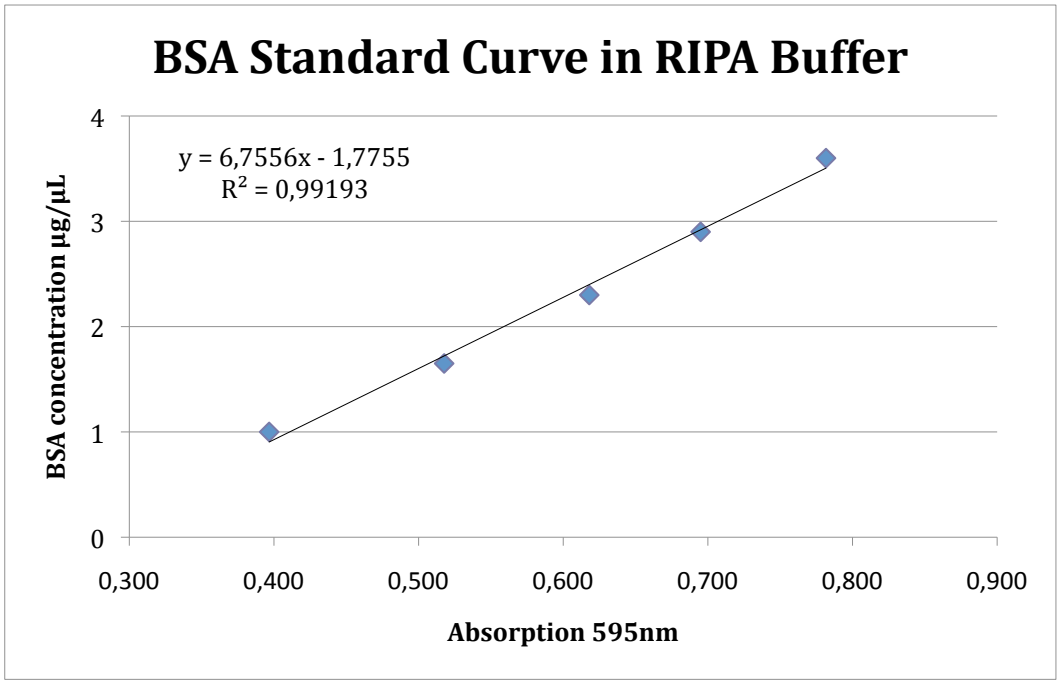

Sample preparation: Concentration of lysates was calculated according to the standard curve described above and set to 2-5µg/µl (depending on the sample with the lowest concentration) by adding 5x sample buffer and β-Mercaptoethanol (10% of final vol.) and adjusting the volume with RIPA buffer. The samples were then boiled at 95°C for 10 min, centrifuged shortly and stored at -20°C.

5x sample buffer (for SDS-PAGE): 320mM Tris HCl, 5% SDS, 50% Glycerol, 0,5% Bromphenol Blue; pH 6,8, stored at -20°C.

Sodium-Dodecyl-Sulphate-Polyachrylamide Gel Electrophoresis (SDS-PAGE)

SDS gel apparatuses were cleaned, assembled and leakage was assessed with EtOH. Separating and stacking gel solutions were prepared according to the table below. Isopropanol was used to cover the polymerizing separating gel in order to ensure proper horizontal polymerization. After 20 to 30 min, the Isopropanol was removed and the stacking gel was poured on top of the separating gel. A comb with 10 slots for mini gels and 15 slots for midi gels was inserted and the stacking gel was left to polymerize for 15 to 20 min. For electrophoresis, the gels were covered with 1x running buffer and samples were loaded with loading tips. Pre-stained protein ladder was used to determine the approximate protein size (PageRuler™ Fermentas Ref. # SM0671, 10µl for mini gel, 20 µl for midi gel). Empty slots were filled with 10µl of 3x sample buffer to avoid any irregularities during the run. Electrophoresis was started with 50V and increased to 100V as soon as the samples entered the separating gel.

Separating gel	mini gel (1,5 mm)	midi gel (1,5 mm)
H_20	4,0 ml	15,8 ml
30% Acrylamid	3,3 ml	13,3ml
1,5 M Tris pH 8,8 + 0,4% SDS	2,5 ml	10,0 ml
10% SDS	0,1 ml	0,4 ml
10% APS	0,1 ml	0,4 ml
TEMED (Tetramethylethylenediamine)	10,0 µl	20,0 µl

Stacking gel	mini gel (1,5 mm)	midi gel (1,5 mm)
H20	2,80 ml	8,40 ml
30% Acrylamid	0,83 ml	2,50 ml
1,5 M Tris pH 6,8 + 0,4% SDS	1,50 ml	3,70 ml
10% SDS	0,05 ml	0,15 ml
10% APS	0,05 ml	0,15 ml
TEMED	5,00 µl	15,00 µl

4x Separating buffer: 1,5 M Tris pH 8,8 + 0,4% SDS
4x Stacking buffer: 0,5 M Tris pH 6,8 + 0,4% SDS
10x Running buffer: 250mM Tris, 2,5M Glycine, 1% SDS
Electrophoresis time: mini gel ~2h-2,5h, midi gel ~4h-4,5h

Western Blot

After electrophoresis, the proteins were blotted onto a nitrocellulose membrane by two different methods: tank transfer and semidry transfer.

Nitrocellulose membranes and Whatman® paper were cut to the approximate size of the gels and pre-wet in transfer buffer before assembly in BioRad Trans blot cell for tank transfer and BioRad Trans-blot Semidry transfer cell for semidry transfer.

Cathode
2 Whatman® papers
gel
nitrocellulose membrane
2 Whatman® papers
Anode

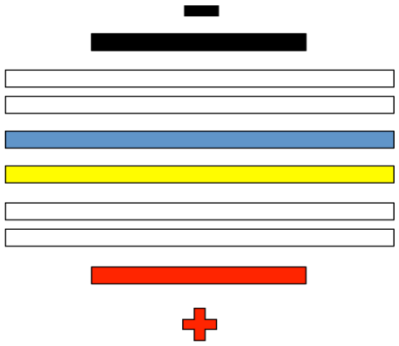

Air bubbles were removed by gently rolling a test tube on the top Whatman® papers.

Semidry transfer (used for mini gels)	45 min	18V
Wet transfer (used for midi gels)	1h	10V
	o/n	30V
	1h	50V

Semidry transfer buffer: 48mM Tris pH 9,2, 39mM glycine, , 0,037%, 20% Methanol

Wet transfer buffer: 25mM Tris pH 8,3, 250 mM glycine, 0,1% SDS, 10% Methanol

Nitrocellulose membrane: Hybond™-C Extra Ref. # RPN303E

Ponceau Red staining: Nitrocellulose membranes were placed in Ponceau Red solution (0,2% Ponceau S, 3% Trichloracetic acid) for one to two minutes and washed with ddH_20 until protein bands became visible. Membranes were scanned and cut into strips aligning to the protein ladder. Finally, membranes were washed 2x for 10 min with TBS-T to remove the remaining Ponceau Red in the membrane.

Immunolabeling: Nitrocellulose membranes were blocked for 1h in 5% milk (non fat milk, powder) in TBS-T, washed 3x with TBS-T for 10 min and incubated with 5-10 ml of primary antibody (see table below) overnight at 4°C rotating. On the next day, membranes were washed 3x with TBS-T for 10 min and incubated with secondary antibody for 1h at RT gently shaking. Membranes were then washed 3x with TBS-T and developed using ECL system (see below).

Antibodies:

primary antibodies:	Epitope	Dilution	Source	MW (kDa)	Company
anti-c-Raf	total protein	1:1000 B[1]	Rabbit, pc[3]	65 – 75	CS[5] #9422
anti-phospho-p44/42 MAP Kinase	Thr202/Tyr 204	1:1000 B[1]	Rabbit, pc[3]	42, 44	CS[5] #9101
anti-posphoStat3	Tyr 705	1:1000 B[1]	Rabbit, mc[4]	79, 86	CS[5] #9145
anti-Tubulin	total protein	1:10000 M[2]	Mouse, mc[4]	55	S-A[6] T9026
anti-YAP	total protein	1:800 B[1]	Rabbit, pc[3]	65 – 75	CS[5] #4912

secondary antibodies:	Dilution	Source	Company
ECL™ anti-rabbit IgG HRP-linked	1:2000 M[2]	donkey	GE Healthcare # NA934V
ECL™ anti-mouse IgG HRP-linked	1:4000 M[2]	sheep	GE Healthcare # NA931V

[1] B: diluted in 3% BSA in TBS-T

[2] M: diluted in 5% Milk (non-fat milk, powder)

[3] poly-clonal

[4] mono-clonal

[5] Cell Signaling Technology®

[6] Sigma- Aldrich Inc.

ECL (Enhanced Chemi-Luminescent) reaction: After immunolabeling, nitrocellulose membranes were incubated in SuperSignal® West Pico Chemiluminescent Substrate (Thermo Scientific, Ref. #34080) for 5 min. Chemiluminscence was detected using Amersham Hyperfilms™ ECL (GE Healthcare, Ref. #28906837) using diverse exposures times ranging from 1

sec to 30 min, depending on signal intensity. Films were developed using a Curix 60 processor (Agfa).

Membrane Stripping

Stripping nitrocellulose membranes is the process by which secondary and primary antibodies are detached from the targeted epitopes. Stripping allows reprobing the membrane with antibodies detecting proteins of similar molecular weights, although loss of total protein amount needs to be taken into consideration. A mild stripping buffer was used for stripping membranes.

Mild stripping buffer: 200mM Glycin, 200mM NaCl, pH 2,5, 3x 30 min at RT gently shacking and 3x 10 min washing with TBS-T.

VI.7 General Solutions and Reagents

Loading buffer (6x):	Bormphenolblue 0,25%, Xylene cyanol FF 0,25% Glycerol 50%, in H20
PBS (Phosphate buffered saline):	137mM NaCL, 2,7mM KCl, 10mM Na_2HPO_4, 1,76mM KH_2PO_4, pH7,4
TAE (50x):	2M Tris, 1M Acetic acid, 0,05M EDTA pH 8
TBS (Tris-Buffered Saline):	25mM, 150mM NaCl, pH 8.
TBS-T (TBS-Tween 0,1%):	25mM, 150mM NaCl, pH 8, 0,01% Tween20

VII. Acknowledgments

Writing this part of my thesis brings up weird feelings and the bitter taste of good-bye. It is time to recall the occurrences of one year, the first time to lay back and think about all the people who have shared a year of their life with me - every single day of it - thank you guys!

Even an acknowledgements section can pose some sort of challenge; there is always the question of whom to start with. My parents? My partner? My boss? My friends? I have decided to keep with my antecessors:

First of all, I would like to thank **Manuela** for this interesting and puzzling project, for her tireless enthusiasm in science, the discussions, her help and her encouragement – until the very last minute!

Thanks to all the Baccarini Boys 'n' Girls for taking me as I am and making me feel comfortable. We have become more than just colleagues. In particular I would like to thank: **Gabriele** for her help and supervision, for forcing me to think before I ask and to articulate myself in the most accurate way and for supporting me up to this point; **Reiner** – were shall I start – for all the oafishness (I mean that in the most positive way possible), the boy's fights in the hallway, his kindness, blitheness and, most importantly, his friendship; **Bartek** for his honesty (which sometimes can be tough), his friendship and for his SSDD attitude; **Josi** for becoming something close to a little sister – although she is older than me – and for all the shoe talk; **Ines** for crossing the line every single day and for her attitude; **Florian** for his sarcasm and candid help; **Babsn** for never stopping to party (the Baccarini Lab has to be represented by someone honorable during Happy Hours!) and for taking care of "my" bench; **Anna** for pushing my Italian every day and productive discussions; **Veronika** for her pleasentness; **Karina** for everlasting sympathy, all the long talks, the cheering up and for sharing deep thoughts; **Katka** for making me believe that one day I might be able to be as disciplined as she is; **Federica** for a great Xmas after-party with a lot of Mojitos

and all the emotions she spread around; **Theó** for bringing the French flair into the lab, for her enthusiasm and straight forwardness. **Clemens** for his freshness and for being the only Austrian that I know who supports the Italian soccer team; **Matthias** for helping me with solutions and for letting me think back to the times of my civil service at the Red Cross; and **Birgit** for being like a fairy godmother to all of us.

Furthermore, I would like to thank the whole Decker's and Kovarik's labs for a great hallway atmosphere, especially **Sebastian** for making me feel slow and lame – thank you – **Bella, Renate, Lisa**, **Ivi**, **Asha** and **Nina** for flirting with me every day, and **Franz** for turning out to be a warm and kindly person.

I would also like to thank all of my dear friends for their patience and understanding, in particular **Christoph** for his friendship, when hard times started to drive me crazy ("easy, easy!"); **Karl** for showing me, like Sebastian, that I am lame and **EGG** for NOT letting me feel lame, my **Monday-lunch-misters, Nicole, Caro, Johannes and Georgi**, my band **Zoeycide (Peter, Lev and Martin)** for quick and intense time-outs, and all the others who I forgot to mention, but are part of my life nonetheless.

Un inimmaginabile GRAZIE a **Mamma** é **Babu** per tutto! Genitori migliori voi non sarebbero da immaginare! Grazie per tutto il vostro supporto morale ed economico. Grazie per avermi sempre lasciato la libertà di fare le mie scelte! Infine grazie a mia sorella **Stephanie** per essere come é.

Last but not least, I would like to thank my significant other **Helene** for supporting, understanding, motivating, loving and sharing her life with me.

VIII. References

ADAMS, D. H. and B. EKSTEEN (2006). "Aberrant homing of mucosal T cells and extra-intestinal manifestations of inflammatory bowel disease." Nat Rev Immunol 6(3): 244-251.

BACCARINI, M. (2005). "Second nature: biological functions of the Raf-1 "kinase"." FEBS Lett 579(15): 3271-3277.

BARNIER, J. V., C. PAPIN, A. EYCHENE, O. LECOQ and G. CALOTHY (1995). "The mouse B-raf gene encodes multiple protein isoforms with tissue-specific expression." J Biol Chem 270(40): 23381-23389.

BERASAIN, C., J. CASTILLO, M. J. PERUGORRIA, M. U. LATASA, J. PRIETO and M. A. AVILA (2009). "Inflammation and liver cancer: new molecular links." Ann N Y Acad Sci 1155: 206-221.

BOHM, F., U. A. KOHLER, T. SPEICHER and S. WERNER (2010). "Regulation of liver regeneration by growth factors and cytokines." EMBO Mol Med 2(8): 294-305.

BUCHMANN, A., R. BAUER-HOFMANN, J. MAHR, N. R. DRINKWATER, A. LUZ and M. SCHWARZ (1991). "Mutational activation of the c-Ha-ras gene in liver tumors of different rodent strains: correlation with susceptibility to hepatocarcinogenesis." Proc Natl Acad Sci U S A 88(3): 911-915.

CASAR, B., A. PINTO and P. CRESPO (2008). "Essential role of ERK dimers in the activation of cytoplasmic but not nuclear substrates by ERK-scaffold complexes." Mol Cell 31(5): 708-721.

CATALANOTTI, F., G. REYES, V. JESENBERGER, G. GALABOVA-KOVACS, R. DE MATOS SIMOES, O. CARUGO and M. BACCARINI (2009). "A Mek1-Mek2 heterodimer determines the strength and duration of the Erk signal." Nat Struct Mol Biol 16(3): 294-303.

CEKANOVA, M., M. MAJIDY, T. MASI, H. A. AL-WADEI and H. M. SCHULLER (2007). "Overexpressed Raf-1 and phosphorylated cyclic adenosine 3'-5'-monophosphatate response element-binding protein are early markers for lung adenocarcinoma." Cancer 109(6): 1164-1173.

CHANG, L. and M. KARIN (2001). "Mammalian MAP kinase signalling cascades." Nature 410(6824): 37-40.

CHEN, A. P., M. OHNO, K. P. GIESE, R. KUHN, R. L. CHEN and A. J. SILVA (2006). "Forebrain-specific knockout of B-raf kinase leads to deficits in hippocampal long-term potentiation, learning, and memory." J Neurosci Res 83(1): 28-38.

CHEN, J., K. FUJII, L. ZHANG, T. ROBERTS and H. FU (2001). "Raf-1 promotes cell survival by antagonizing apoptosis signal-regulating kinase 1 through a MEK-ERK independent mechanism." Proc Natl Acad Sci U S A 98(14): 7783-7788.

CRESSMAN, D. E., L. E. GREENBAUM, R. A. DEANGELIS, G. CILIBERTO, E. E. FURTH, V. POLI and R. TAUB (1996). "Liver failure and defective hepatocyte regeneration in interleukin-6-deficient mice." Science 274(5291): 1379-1383.

DAVIES, H., G. R. BIGNELL, C. COX, P. STEPHENS, S. EDKINS, S. CLEGG, J. TEAGUE, H. WOFFENDIN, M. J. GARNETT, W. BOTTOMLEY, N. DAVIS, E. DICKS, R. EWING, Y. FLOYD, K. GRAY, S. HALL, R. HAWES, J. HUGHES, V. KOSMIDOU, A. MENZIES, C. MOULD, A. PARKER, C. STEVENS, S. WATT, S. HOOPER, R. WILSON, H. JAYATILAKE, B. A. GUSTERSON, C. COOPER, J. SHIPLEY, D. HARGRAVE, K. PRITCHARD-JONES, N. MAITLAND, G. CHENEVIX-TRENCH, G. J. RIGGINS, D. D. BIGNER, G. PALMIERI, A. COSSU, A. FLANAGAN, A. NICHOLSON, J. W. HO, S. Y. LEUNG, S. T. YUEN, B. L. WEBER, H. F. SEIGLER, T. L. DARROW, H. PATERSON, R. MARAIS, C. J. MARSHALL, R. WOOSTER, M. R. STRATTON and P. A. FUTREAL (2002). "Mutations of the BRAF gene in human cancer." Nature 417(6892): 949-954.

DING, J., Y. FENG and H. Y. WANG (2007). "From cell signaling to cancer therapy." Acta Pharmacol Sin 28(9): 1494-1498.

EHRENREITER, K., F. KERN, V. VELAMOOR, K. MEISSL, G. GALABOVA-KOVACS, M. SIBILIA and M. BACCARINI (2009). "Raf-1 addiction in Ras-induced skin carcinogenesis." Cancer Cell 16(2): 149-160.

EHRENREITER, K., D. PIAZZOLLA, V. VELAMOOR, I. SOBCZAK, J. V. SMALL, J. TAKEDA, T. LEUNG and M. BACCARINI (2005). "Raf-1 regulates Rho signaling and cell migration." J Cell Biol 168(6): 955-964.

FARAZI, P. A. and R. A. DEPINHO (2006). "Hepatocellular carcinoma pathogenesis: from genes to environment." Nat Rev Cancer 6(9): 674-687.

FAUSTO, N., J. S. CAMPBELL and K. J. RIEHLE (2006). "Liver regeneration." Hepatology 43(2 Suppl 1): S45-53.

GALABOVA-KOVACS, G., F. CATALANOTTI, D. MATZEN, G. X. REYES, J. ZEZULA, R. HERBST, A. SILVA, I. WALTER and M. BACCARINI (2008). "Essential role of B-Raf in oligodendrocyte maturation and myelination during postnatal central nervous system development." J Cell Biol 180(5): 947-955.

GALABOVA-KOVACS, G., D. MATZEN, D. PIAZZOLLA, K. MEISSL, T. PLYUSHCH, A. P. CHEN, A. SILVA and M. BACCARINI (2006). "Essential role of B-Raf in ERK activation during extraembryonic development." Proc Natl Acad Sci U S A 103(5): 1325-1330.

GARNETT, M. J., S. RANA, H. PATERSON, D. BARFORD and R. MARAIS (2005). "Wild-type and mutant B-RAF activate C-RAF through distinct mechanisms involving heterodimerization." Mol Cell 20(6): 963-969.

GRAVES, M. (2000). Cancer: The Evolutionary Legacy. London, Springer.

HANAHAN, D. and R. A. WEINBERG (2000). "The hallmarks of cancer." Cell 100(1): 57-70.

HATTORI, K., I. NAGURO, C. RUNCHEL and H. ICHIJO (2009). "The roles of ASK family proteins in stress responses and diseases." Cell Commun Signal 7: 9.

HEINDRYCKX, F., I. COLLE and H. VAN VLIERBERGHE (2009). "Experimental mouse models for hepatocellular carcinoma research." Int J Exp Pathol 90(4): 367-386.

HINDLEY, A. and W. KOLCH (2002). "Extracellular signal regulated kinase (ERK)/mitogen activated protein kinase (MAPK)-independent functions of Raf kinases." J Cell Sci 115(Pt 8): 1575-1581.

HOLT, M. P. and C. JU (2006). "Mechanisms of drug-induced liver injury." AAPS J 8(1): E48-54.

HOPFNER, M., D. SCHUPPAN and H. SCHERUBL (2008). "Growth factor receptors and related signalling pathways as targets for novel treatment strategies of hepatocellular cancer." World J Gastroenterol 14(1): 1-14.

HUI, L., K. ZATLOUKAL, H. SCHEUCH, E. STEPNIAK and E. F. WAGNER (2008). "Proliferation of human HCC cells and chemically induced mouse liver cancers requires JNK1-dependent p21 downregulation." J Clin Invest 118(12): 3943-3953.

HUSER, M., J. LUCKETT, A. CHILOECHES, K. MERCER, M. IWOBI, S. GIBLETT, X. M. SUN, J. BROWN, R. MARAIS and C. PRITCHARD (2001). "MEK kinase activity is not necessary for Raf-1 function." EMBO J 20(8): 1940-1951.

HUYNH, H., T. T. NGUYEN, K. H. CHOW, P. H. TAN, K. C. SOO and E. TRAN (2003). "Over-expression of the mitogen-activated protein kinase (MAPK) kinase (MEK)-MAPK in hepatocellular carcinoma: its role in tumor progression and apoptosis." BMC Gastroenterol 3: 19.

HWANG, Y. H., J. Y. CHOI, S. KIM, E. S. CHUNG, T. KIM, S. S. KOH, B. LEE, S. H. BAE, J. KIM and Y. M. PARK (2004). "Over-expression of c-raf-1 proto-oncogene in liver cirrhosis and hepatocellular carcinoma." Hepatol Res 29(2): 113-121.

IMAOKA, S., M. OSADA, Y. MINAMIYAMA, T. YUKIMURA, S. TOYOKUNI, S. TAKEMURA, T. HIROI and Y. FUNAE (2004). "Role of phenobarbital-inducible cytochrome P450s as a source of active oxygen species in DNA-oxidation." Cancer Lett 203(2): 117-125.

ITO, Y., S. NAKASHIMA and Y. NOZAWA (1998). "Possible involvement of mitogen-activated protein kinase in phospholipase D activation induced by H2O2, but not by carbachol, in rat pheochromocytoma PC12 cells." J Neurochem 71(6): 2278-2285.

KANG, J. S., H. WANIBUCHI, K. MORIMURA, F. J. GONZALEZ and S. FUKUSHIMA (2007). "Role of CYP2E1 in diethylnitrosamine-induced hepatocarcinogenesis in vivo." Cancer Res 67(23): 11141-11146.

KELLENDONK, C., C. OPHERK, K. ANLAG, G. SCHUTZ and F. TRONCHE (2000). "Hepatocyte-specific expression of Cre recombinase." Genesis 26(2): 151-153.

KOLCH, W. (2000). "Meaningful relationships: the regulation of the Ras/Raf/MEK/ERK pathway by protein interactions." Biochem J 351 Pt 2: 289-305.

KUHN, R., F. SCHWENK, M. AGUET and K. RAJEWSKY (1995). "Inducible gene targeting in mice." Science 269(5229): 1427-1429.

LEE, J. S., I. S. CHU, A. MIKAELYAN, D. F. CALVISI, J. HEO, J. K. REDDY and S. S. THORGEIRSSON (2004). "Application of comparative functional genomics to identify best-fit mouse models to study human cancer." Nat Genet 36(12): 1306-1311.

LIN, W. W. and M. KARIN (2007). "A cytokine-mediated link between innate immunity, inflammation, and cancer." J Clin Invest 117(5): 1175-1183.

MAEDA, S., H. KAMATA, J. L. LUO, H. LEFFERT and M. KARIN (2005). "IKKbeta couples hepatocyte death to cytokine-driven compensatory proliferation that promotes chemical hepatocarcinogenesis." Cell 121(7): 977-990.

MARAIS, R., Y. LIGHT, H. F. PATERSON, C. S. MASON and C. J. MARSHALL (1997). "Differential regulation of Raf-1, A-Raf, and B-Raf by oncogenic ras and tyrosine kinases." J Biol Chem 272(7): 4378-4383.

MARTIN, G. S. (2003). "Cell signaling and cancer." Cancer Cell 4(3): 167-174.

MATALLANAS, D., D. ROMANO, K. YEE, K. MEISSL, L. KUCEROVA, D. PIAZZOLLA, M. BACCARINI, J. K. VASS, W. KOLCH and E. O'NEILL (2007). "RASSF1A elicits apoptosis through an MST2 pathway directing proapoptotic transcription by the p73 tumor suppressor protein." Mol Cell 27(6): 962-975.

METZGER, C. (2004). "Cre-mediated conditional gene targeting to understand liver functions." Drug Discovery Today: Disease Models 1(3): 229-234

MIKULA, M., M. SCHREIBER, Z. HUSAK, L. KUCEROVA, J. RUTH, R. WIESER, K. ZATLOUKAL, H. BEUG, E. F. WAGNER and M. BACCARINI (2001). "Embryonic lethality and fetal liver apoptosis in mice lacking the c-raf-1 gene." EMBO J 20(8): 1952-1962.

MORICE, C., F. NOTHIAS, S. KONIG, P. VERNIER, M. BACCARINI, J. D. VINCENT and J. V. BARNIER (1999). "Raf-1 and B-Raf proteins have similar regional distributions but differential subcellular localization in adult rat brain." Eur J Neurosci 11(6): 1995-2006.

NAKATANI, T., G. ROY, N. FUJIMOTO, T. ASAHARA and A. ITO (2001). "Sex hormone dependency of diethylnitrosamine-induced liver tumors in mice and chemoprevention by leuprorelin." Jpn J Cancer Res 92(3): 249-256.

NAUGLER, W. E., T. SAKURAI, S. KIM, S. MAEDA, K. KIM, A. M. ELSHARKAWY and M. KARIN (2007). "Gender disparity in liver cancer due to sex differences in MyD88-dependent IL-6 production." Science 317(5834): 121-124.

NIAULT, T. (2009). Raf Kinases in the Mouse Epidermis. Department of Microbiology and Immunobiology. Vienna, AUT, University of Vienna.

NIAULT, T. S. and M. BACCARINI (2010). "Targets of Raf in tumorigenesis." Carcinogenesis 31(7): 1165-1174.

O'NEILL, E., L. RUSHWORTH, M. BACCARINI and W. KOLCH (2004). "Role of the kinase MST2 in suppression of apoptosis by the proto-oncogene product Raf-1." Science 306(5705): 2267-2270.

OLIVEIRA, P. A., A. COLACO, R. CHAVES, H. GUEDES-PINTO, P. L. DE-LA-CRUZ and C. LOPES (2007). "Chemical carcinogenesis." An Acad Bras Cienc 79(4): 593-616.

ORTON, R. J., O. E. STURM, V. VYSHEMIRSKY, M. CALDER, D. R. GILBERT and W. KOLCH (2005). "Computational modelling of the receptor-tyrosine-kinase-activated MAPK pathway." Biochem J 392(Pt 2): 249-261.

PAN, D. (2010). "The hippo signaling pathway in development and cancer." Dev Cell 19(4): 491-505.

PARK, D. H., J. W. SHIN, S. K. PARK, J. N. SEO, L. LI, J. J. JANG and M. J. LEE (2009). "Diethylnitrosamine (DEN) induces irreversible hepatocellular carcinogenesis through overexpression of G1/S-phase regulatory proteins in rat." Toxicol Lett 191(2-3): 321-326.

PARK, E. J., J. H. LEE, G. Y. YU, G. HE, S. R. ALI, R. G. HOLZER, C. H. OSTERREICHER, H. TAKAHASHI and M. KARIN (2010). "Dietary and genetic obesity promote liver inflammation and tumorigenesis by enhancing IL-6 and TNF expression." Cell 140(2): 197-208.

PARKIN, D. M., F. BRAY, J. FERLAY and P. PISANI (2001). "Estimating the world cancer burden: Globocan 2000." Int J Cancer 94(2): 153-156.

PIAZZOLLA, D., K. MEISSL, L. KUCEROVA, C. RUBIOLO and M. BACCARINI (2005). "Raf-1 sets the threshold of Fas sensitivity by modulating Rok-alpha signaling." J Cell Biol 171(6): 1013-1022.

PRITCHARD, C. A., L. BOLIN, R. SLATTERY, R. MURRAY and M. MCMAHON (1996). "Post-natal lethality and neurological and gastrointestinal defects in mice with targeted disruption of the A-Raf protein kinase gene." Curr Biol 6(5): 614-617.

PRITCHARD, C. A., M. L. SAMUELS, E. BOSCH and M. MCMAHON (1995). "Conditionally oncogenic forms of the A-Raf and B-Raf protein kinases display different biological and biochemical properties in NIH 3T3 cells." Mol Cell Biol 15(11): 6430-6442.

RAJEWSKY, K., H. GU, R. KUHN, U. A. BETZ, W. MULLER, J. ROES and F. SCHWENK (1996). "Conditional gene targeting." J Clin Invest 98(3): 600-603.

RAO, K. V. and S. D. VESSELINOVITCH (1973). "Age- and sex-associated diethylnitrosamine dealkylation activity of the mouse liver and hepatocarcinogenesis." Cancer Res 33(7): 1625-1627.

RIVA, C., J. P. LAVIEILLE, E. REYT, E. BRAMBILLA, J. LUNARDI and C. BRAMBILLA (1995). "Differential c-myc, c-jun, c-raf and p53 expression in squamous cell carcinoma of the head and neck: implication in drug and radioresistance." Eur J Cancer B Oral Oncol 31B(6): 384-391.

ROBERTS, R. A., P. E. GANEY, C. JU, L. M. KAMENDULIS, I. RUSYN and J. E. KLAUNIG (2007). "Role of the Kupffer cell in mediating hepatic toxicity and carcinogenesis." Toxicol Sci 96(1): 2-15.

RUSHWORTH, L. K., A. D. HINDLEY, E. O'NEILL and W. KOLCH (2006). "Regulation and role of Raf-1/B-Raf heterodimerization." Mol Cell Biol 26(6): 2262-2272.

SAKAMOTO, T., Z. LIU, N. MURASE, T. EZURE, S. YOKOMURO, V. POLI and A. J. DEMETRIS (1999). "Mitosis and apoptosis in the liver of interleukin-6-deficient mice after partial hepatectomy." Hepatology 29(2): 403-411.

SOBCZAK, I., G. GALABOVA-KOVACS, I. SADZAK, A. KREN, G. CHRISTOFORI and M. BACCARINI (2008). "B-Raf is required for ERK activation and tumor progression in a mouse model of pancreatic beta-cell carcinogenesis." Oncogene 27(35): 4779-4787.

STIENSTRA, R., F. SAUDALE, C. DUVAL, S. KESHTKAR, J. E. GROENER, N. VAN ROOIJEN, B. STAELS, S. KERSTEN and M. MULLER (2010). "Kupffer cells promote hepatic steatosis via interleukin-1beta-dependent suppression of peroxisome proliferator-activated receptor alpha activity." Hepatology 51(2): 511-522.

TANNAPFEL, A., F. SOMMERER, M. BENICKE, A. KATALINIC, D. UHLMANN, H. WITZIGMANN, J. HAUSS and C. WITTEKIND (2003). "Mutations of the BRAF gene in cholangiocarcinoma but not in hepatocellular carcinoma." Gut 52(5): 706-712.

TAUB, R. (2004). "Liver regeneration: from myth to mechanism." Nat Rev Mol Cell Biol 5(10): 836-847.

TEOH, N. C., Y. Y. DAN, K. SWISSHELM, S. LEHMAN, J. H. WRIGHT, J. HAQUE, Y. GU and N. FAUSTO (2008). "Defective DNA strand break repair causes chromosomal instability and accelerates liver carcinogenesis in mice." Hepatology 47(6): 2078-2088.

THIEL, G., M. EKICI and O. G. ROSSLER (2009). "Regulation of cellular proliferation, differentiation and cell death by activated Raf." Cell Commun Signal 7: 8.

THOMAS, M. B. and J. L. ABBRUZZESE (2005). "Opportunities for targeted therapies in hepatocellular carcinoma." J Clin Oncol 23(31): 8093-8108.

TOFFANIN, S., S. L. FRIEDMAN and J. M. LLOVET (2010). "Obesity, inflammatory signaling, and hepatocellular carcinoma-an enlarging link." Cancer Cell 17(2): 115-117.

TSUKAMOTO, H., A. IRIE, S. SENJU, A. K. HATZOPOULOS, L. WOJNOWSKI and Y. NISHIMURA (2008). "B-Raf-mediated signaling pathway regulates T cell development." Eur J Immunol 38(2): 518-527.

VERNA, L., J. WHYSNER and G. M. WILLIAMS (1996). "N-nitrosodiethylamine mechanistic data and risk assessment: bioactivation, DNA-adduct formation, mutagenicity, and tumor initiation." Pharmacol Ther 71(1-2): 57-81.

VESSELINOVITCH, S. D. and N. MIHAILOVICH (1983). "Kinetics of diethylnitrosamine hepatocarcinogenesis in the infant mouse." Cancer Res 43(9): 4253-4259.

VETELAINEN, R., A. K. VAN VLIET and T. M. VAN GULIK (2007). "Severe steatosis increases hepatocellular injury and impairs liver regeneration in a rat model of partial hepatectomy." Ann Surg 245(1): 44-50.

WATSON, R. E. and J. I. GOODMAN (2002). "Effects of phenobarbital on DNA methylation in GC-rich regions of hepatic DNA from mice that exhibit different levels of susceptibility to liver tumorigenesis." Toxicol Sci 68(1): 51-58.

WAXMAN, D. J. and L. AZAROFF (1992). "Phenobarbital induction of cytochrome P-450 gene expression." Biochem J 281 (Pt 3): 577-592.

WEBER, C. K., J. R. SLUPSKY, H. A. KALMES and U. R. RAPP (2001). "Active Ras induces heterodimerization of cRaf and BRaf." Cancer Res 61(9): 3595-3598.

WELLBROCK, C., M. KARASARIDES and R. MARAIS (2004). "The RAF proteins take centre stage." Nat Rev Mol Cell Biol 5(11): 875-885.

WHITTAKER, S., R. MARAIS and A. X. ZHU (2010). "The role of signaling pathways in the development and treatment of hepatocellular carcinoma." Oncogene 29(36): 4989-5005.

WHO. (2009). "Cancer." from http://www.who.int/mediacentre/factsheets/fs297/en/index.html.

WOJNOWSKI, L., L. F. STANCATO, A. C. LARNER, U. R. RAPP and A. ZIMMER (2000). "Overlapping and specific functions of Braf and Craf-1 proto-oncogenes during mouse embryogenesis." Mech Dev 91(1-2): 97-104.

WONG, C. C., C. M. WONG, F. C. KO, L. K. CHAN, Y. P. CHING, J. W. YAM and I. O. NG (2008). "Deleted in liver cancer 1 (DLC1) negatively regulates Rho/ROCK/MLC pathway in hepatocellular carcinoma." PLoS One 3(7): e2779.

YAMAGUCHI, O., T. WATANABE, K. NISHIDA, K. KASHIWASE, Y. HIGUCHI, T. TAKEDA, S. HIKOSO, S. HIROTANI, M. ASAHI, M. TANIIKE, A. NAKAI, I. TSUJIMOTO, Y. MATSUMURA, J. MIYAZAKI, K. R. CHIEN, A. MATSUZAWA, C. SADAMITSU, H. ICHIJO, M. BACCARINI, M. HORI and K. OTSU (2004). "Cardiac-specific disruption of the c-raf-1 gene induces cardiac dysfunction and apoptosis." J Clin Invest 114(7): 937-943.

YOON, S. and R. SEGER (2006). "The extracellular signal-regulated kinase: multiple substrates regulate diverse cellular functions." Growth Factors 24(1): 21-44.

ZENDER, L., M. S. SPECTOR, W. XUE, P. FLEMMING, C. CORDON-CARDO, J. SILKE, S. T. FAN, J. M. LUK, M. WIGLER, G. J. HANNON, D. MU, R. LUCITO, S. POWERS and S. W. LOWE (2006). "Identification and validation of oncogenes in liver cancer using an integrative oncogenomic approach." Cell 125(7): 1253-1267.

IX. Curriculum Vitae

Personal Information

Name:	Matthias Parrini
Address:	Hofgartenstr 6, 2100 Leobendorf
Telephone:	+43 (0)699 10 69 64 62
Email:	matthias.parrini@gmail.com
Date of Birth:	11-28-1983
Place of Birth	Vienna, Austria
Citizenship:	Austrian, Italian

Academic studies

since 10/2004	Studies of Molecular Biology at the University of Vienna focuses on cell biology, immunology and molecular medicine Further lab experience in biochemistry, genetics, microbiology, cell biology as well as analytic and organic chemistry.
08 – 09/2008	Internship at MFPL – Max F. Perutz Laboratories, Prof. Wiche lab – cell biology, membranes and the cytoskeleton
11 – 12/2008	Internship at MFPL – Max F. Perutz Laboratories, Prof. Dr. Baccarini lab – cell signaling, MAPK signaling cascade
03 – 04/2009	Internship at Medical University of Vienna, Michelle Epstein M.D. – immunology, experimental allergy
06/2009 – 08/2010	Diploma thesis at MFPL – Max F. Perutz Laboratories, Prof. Dr. Baccarini lab – cell signaling, MAPK signaling in Cancer

Civil Service and Voluntary Work

10/2003 – 09/2004	Paramedic at the Red Cross Korneuburg/Stockerau/Ernstbrunn
since 10/2004	voluntary assistance as Paramedic at the Red Cross Korneuburg/Stockerau/Ernstbrunn

Education

06/2003	graduation, passed with distinction
09/1998 – 06/2003	Commercial Academy (Handelsakademie) Korneuburg, Lower Austria
09/1997 – 06/1998	Secondary School Korneuburg, Lower Austria
09/1994 – 06/1997	Grammer School Stockerau, Lower Austria
09/1990 – 06/1994	Primary School Leobendorf, Lower Austria

Representative Work

11/2006 – 09/2007	Member of the Senat, University of Vienna
09/2002 – 09/2003	Head of School Council at the Commercial Academy Korneuburg
09/1998 – 09/2000	Class Representative at the Commercial Academy Korneuburg

Employment History

Since 08/2001	Firma Schnabl GesmbH & CoKG, administration assistant
06/2007 – 09/2009	Kite 2 Fly - Podersdorf, kitesurfing teacher

Language Education

Native Language	German
Foreign Languages	English (fluent)
	Italian (fluent)
	French (intermediate)

11/2002	Certificate of Business English (ESOL) – University of Cambridge
01 – 07/2001	high school exchange year in Hinton Gerard Redmond Community Catholic School, Alberta, Canada
08/1998	English language summer school, Plymouth, Great Britain
08/1999	English language summer school, Arklow, Ireland
08/2000	French language summer school, Biarritz, France
09/1991 – 06/1997	Italian language school in Vienna – Italian ministry for foreign affairs

Personal Interests music, kitesurfing, ice hockey, mountain biking

Vienna, 1st of November 2010 Matthias Parrini